REPUBLIC OF TÜRKİYE
YILDIZ TECHNICAL UNIVERSITY
GRADUATE SCHOOL OF SCIENCE AND ENGINEERING

INVESTIGATION OF SHEAR STRENGTH OF SOILS WITH DIFFERENT SATURATION DEGREES

Safi Nashat Safi ALJALIL

MASTER OF SCIENCE THESIS

Department of Civil Engineering

Program of Geotechnical Engineering

Supervisor

Asst. Prof. Dr. Murat Ergenokon SELÇUK

August, 2024

REPUBLIC OF TÜRKİYE

YILDIZ TECHNICAL UNIVERSITY

GRADUATE SCHOOL OF SCIENCE AND ENGINEERING

INVESTIGATION OF SHEAR STRENGTH OF SOILS WITH DIFFERENT SATURATION DEGREES

A thesis submitted by Safi Nashat Safi ALJALIL in partial fulfillment of the requirements for the degree of **MASTER OF SCIENCE** is approved by the committee on 07.08.2024 in the Department of Civil Engineering, Program of Geotechnical Engineering.

Asst. Prof. Dr. Murat Ergenokon
SELÇUK
Yıldız Technical University
Supervisor

Approved By the Examining Committee

Asst. Prof. Dr. Murat Ergenokon SELÇUK, Supervisor

Yildiz Technical University _____

Asst. Prof. Dr. Murat TONAROĞLU, Member

Yildiz Technical University _____

Assoc. Prof. Dr. ZÜLAL AKBAY ARAMA, Member

İstanbul University-Cerrahpaşa _____

I hereby declare that I have obtained the required legal permissions during data collection and exploitation procedures, that I have made the in-text citations and cited the references properly, that I haven't falsified and/or fabricated research data and results of the study and that I have abided by the principles of the scientific research and ethics during my Thesis Study under the title of "Investigation Of Shear Strength Of Soils With Different Saturation Degrees" supervised by my supervisor, assist. Prof. Dr. Murat Ergenokon SELÇUK. In the case of a discovery of false statement, I am to acknowledge any legal consequence.

Safi Nashat Safi ALJALIL

Signature

Dedicated To the Purest soul I’ve known,

my loving father

ACKNOWLEDGEMENTS

I would like to acknowledge and give my warmest thanks to my supervisor Assist. Prof. Dr. Murat Ergenokon SELÇUK who made this work possible. His guidance and advice carried me through all the stages of writing my project. I would also like to thank my committee members for letting my defense be an enjoyable moment, and for your brilliant comments and suggestions, thanks to you.

I would like to give my special thanks to my mother, my family, and my uncle Dr. Hikmet for their unwavering support and understanding throughout my research and project writing, my colleagues Nazli and Serdar for their continued support and guidance, and my family in Istanbul that got me through a lot. Your prayers have carried me through to this point.

Lastly, I am grateful to God for guiding me through all the challenges.

Safi Nashat Safi ALJALIL

TABLE OF CONTENTS

LIST OF SYMBOLS

A	Air
c	Cohesion
D_R	Degree of curvature
c'	Drained cohesion
φ'	Drained internal friction angle
ϕ	Internal friction angle
w_{opt}	Optimum water content
k	Permeability
U	Pore pressure
N	Porosity
Dr	Relative density
R	Roundness
S	Saturation
τ	Shear strength
τ_f	Shear stress at failure
Gs	Specific density
Σ	Suction stress
σ'	Total stress
q_u	Unconfined compressive strength
c_u	Undrained shear strength
γ	Unit volume weight
E	Void ratio
ΔV	Volume
w	Water content

LIST OF ABBREVIATIONS

ASTM	American Society for Testing and Materials
DS	Direct shear
PDMS	Polydimethylsiloxane
S	Saturation
SWRC	Soil Water Retention Curve

LIST OF FIGURES

LIST OF TABLES

ABSTRACT

INVESTIGATION OF SHEAR STRENGTH OF SOILS WITH DIFFERENT SATURATION DEGREES

Safi Nashat Safi ALJALIL

Department of Civil Engineering

Master of Science Thesis

Supervisor: Assist. Prof. Dr. Murat Ergenokon SELÇUK

Soil behavior has been the core study of geotechnical research, it has various behaviors based on the composition, particular size and arrangement, grain distribution…etc. This study focuses on the effect of the high saturation degree on granular soil particles. It has an unpredictably great effect on soil grains, saturated soil is considered one of the worst cases in geotechnical engineering. As the soil approaches the full saturation degree, the bonds between the soil particles become stronger, while the bonds become weaker as they move away from the full saturation degree.

The shear strength based on the degree of saturation was investigated. Poorly graded fine sands (SS1) with a relative density of 35% were prepared in different degrees of saturation (Dry, 95%, 90%, 85%, 80%, 75%, 70%, 50%, 25%, and fully saturated). The optimum time required for the soil curing duration has been predetermined. Small-scale direct shear tests were executed on samples that were prepared under 3 different normal stresses (62.5, 125, and 250) kPa where each was repeated 3 times to get the optimum average result as this case is so sensitive. The direct shear tests provided the Peak and residual behavior. Depending on the outcomes of all these experiments to determine the shear parameters from the

failure envelope through the Mohr-Coulomb failure envelope. As a result, shear behavior variations of the fine sands depending on the saturation rate were presented with graphics, and the internal friction angle variation, suction, cohesion, and dilation according to the saturation rate were explained, and it was compared to a different degree of saturation of 65% (SS2) with (Dry, 95%, 90%, 80%, 70%, 50%, 25%, and fully saturated). In addition, the relationship between the degree of saturation and particle arrangement is observed, alongside the soil's particular size was studied with an image analysis technique.

Keywords: Partially saturated, behavioral change, shear strength, cohesion, angle of friction, image analysis

ÖZET

FARKLI SUYA DOYGUNLUK DERECESİNE SAHİP ZEMİNLERİN KAYMA MUKAVEMETİNİN İNCELENMESİ

Safi Nashat Safi ALJALIL

İnşaat Mühendisliği Anabilim Dalı

Yüksek Lisans Tezi

Danışman: Dr. Öğr. Üyesi Murat Ergenokon SELÇUK

Zemin davranışı geoteknik araştırmaların ana çalışması olmuştur ve bileşim, partikül boyutu ve düzeni, tane dağılımı vb. faktörlere bağlı olarak çeşitli davranışlar sergiler. Bu çalışma, yüksek derecede doygunluğun granüler zemin partikülleri üzerindeki etkisine odaklanmaktadır. Doygun zemin, geoteknik mühendisliğinde en kötü durumlardan biri olarak kabul edilir ve zemin taneleri üzerinde öngörülemeyen büyük bir etkiye sahiptir. Zemin tam doygunluk derecesine yaklaştıkça, zemin partikülleri arasındaki bağlar güçlenir, tam doygunluk derecesinden uzaklaştıkça bu bağlar zayıflar.

Doygunluk derecesine bağlı olarak kesme mukavemeti incelenmiştir. 35% rölatif sıkılığa sahip, kötü derecelendirilmiş ince kumlar (SS1), farklı doygunluk derecelerinde (kuru, 95%, 90%, 85%, 80%, 75%, 70%, 50%, 25% ve tam doygun) hazırlanmıştır. Zeminin kürlenme süresi için gerekli optimum süre önceden belirlenmiştir. Hazırlanan numunelere, her biri 3 kez tekrarlanan 3 farklı normal gerilim altında (62.5, 125, and 250) kPa küçük ölçekli kesme kutusu deneyi uygulanmıştır; bu durum çok hassas olduğu için optimum ortalama sonuç elde edilmiştir. Doğrudan kesme testleri, pik ve rezidüel davranış sağlamıştır. Bu

deneylerin sonuçlarına dayanarak, Mohr-Coulomb kırılma zarfından kesme mukavemeti parametreleri belirlenmiştir. Sonuç olarak, ince kumların doygunluk oranına bağlı olarak kesme davranışındaki değişim grafiklerle sunulmuş ve içsel sürtünme açısı, kohezyon, emme ve dilatasyonun doygunluk oranına göre değişimi açıklanmıştır. Ayrıca, 65% (SS2) doygunluk derecesine sahip farklı bir derece ile (kuru, 95%, 90%, 80%, 70%, 50%, 25%, ve tam doygun) karşılaştırılmıştır. Ek olarak, doygunluk derecesi ile partikül düzeni arasındaki ilişki gözlemlenmiş ve partikül boyutu görüntü analizi tekniği ile incelenmiştir.

Anahtar kelimeler: Kısmen doygun, davranış değişikliği, kesme mukavemeti, kohezyon, sürtünme açısı, görüntü analizi

1
INTRODUCTION

1.1 Introduction

The study will investigate the mechanical behavior of highly saturated sand, particularly focusing on the connection between the angle of friction, shear strength, and deformation stress. The mechanical properties will be assessed using a direct shear apparatus to analyze how changes in the saturation degree affect the behavior of sand.

The area of the mechanical behavior's relation with the degree of saturation has affected many geotechnical aspects and engineers are interested to fully covering it. When a soil sample is completely saturated, the voids are filled with water, which resists shear through adhesion and cohesion. However, if the sample is affected by evaporation due to temperature or water leak, the water leaves behind an empty void, which has less pressure than the atmosphere. Particles are pulled, sucked, and stuck together due to suction, which theoretically proves that the shear strength should be stronger.

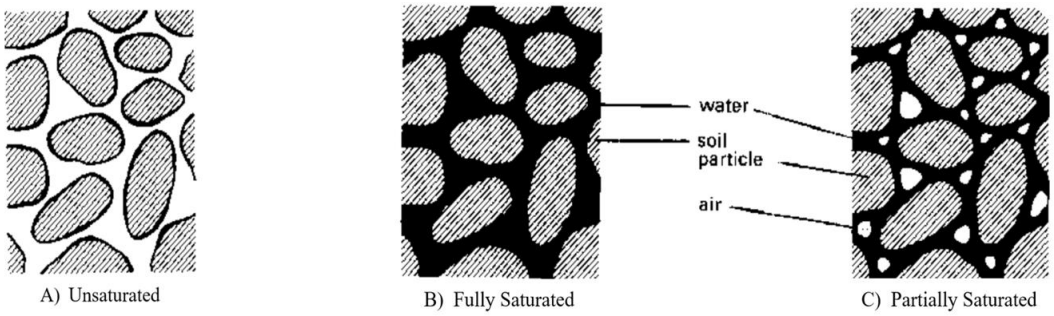

Figure 1.1 Soil moisture characteristics.

Figure 1.1 illustrates various soil compositions in the presence of water. In the fully saturated case (A), the particles are surrounded by water, leaving no vacuum to

cause suction. In the unsaturated case (C), there is no water to create a bridge between the particles, so no air is trapped. In the partially saturated case (B), the water creates a bridge bond between particles, tending to bind them together due to suction caused by the vacuum spaces.

Numerous investigations on the mechanical properties of unsaturated soils have been carried out over time. Since the behavior of unsaturation is predicted to be more clear in fine soils, the majority of these investigations have concentrated on these soil types. In geotechnical fields, the principles and classical ideas of saturated soils are no longer consistent wherever largely unsaturated soils are predominant. Since the amount of water in soils has a significant impact on the behavior of its constituent elements, knowledge regarding the influence of water content on the coupled hydraulic-mechanical behavior is of great relevance for numerous geotechnical concerns. Water affects the stability of structure and the soil strength because it behaves as a binding agent and as a lubricant [1].

1.2 Literature Review

Since saturated soils exhibit a wide range of behaviors that make them difficult to study, many researchers have focused on a small portion of the subject to help other researchers determine which areas to pursue further; the forthcoming chapter will attempt to highlight which areas require further investigation.

The shear strength of a material or component refers to its capacity to endure a lateral load, which causes particles to slide and potentially lead to structural failure. This point of failure, where the structure can no longer resist the load, is defined as the shear strength. To measure soil's shear strength, a direct shear procedure is conducted. During the test, soil is formed into two layers within a direct shear box, and pressure is applied parallelly to each layer. The soil particles resist this applied force, and this resistance is known as shear resistance.

The behavior of soil especially the mechanical one, including sand, and saturation degree significantly influenced it. Here's how the mechanical behavior of partially saturated sand differs from that of fully saturated or dry sand [2,3]:

Fully saturated sand:

- In fully saturated sand, all pore spaces are filled with water, leaving no air

voids.

- The presence of water lubricates the soil particles, reducing interparticle friction and allowing for easier particle movement.
- Fully saturated sand tends to exhibit more uniform and predictable mechanical behavior compared to partially saturated or dry sand.
- Shear strength is generally lower in fully saturated sand due to the reduced effective stress caused by pore water pressure.

Partially saturated sand:

- Partially saturated sand contains both water and air within its pore spaces, with varying degrees of saturation.
- The presence of air voids introduces additional complexity to the soil's mechanical behavior, as it affects the distribution of pore pressures and interparticle forces.
- The soil's shear strength usually increases when the saturation degree drops because of the increased effective stress brought on by the decrease in pore water pressure.
- Partially saturated sand may exhibit non-linear and time-dependent behavior, especially during wetting or drying processes, due to changes in pore water pressure and soil structure.

Dry sand:

- Dry sand contains no pore water and is fully saturated with air.
- Dry sand tends to have higher shear strength compared to partially saturated or fully saturated sand, as there is no pore water to reduce the effective stress.
- However, dry sand is also more susceptible to volume change and contraction during loading because of the absence of pore water pressure.
- Dry sand may exhibit brittle behavior under loading, with little or no deformation before reaching failure.

1.3 Mechanical Characteristics of Partially Saturated Soil

Understanding the mechanical characteristics of unsaturated soil is essential for predicting its behavior under different environmental and loading conditions. There is various factors influencing these characteristics, including shear strength, angle

of friction, grain size distribution, particle distribution, particle shape, packing, effective stress, soil structure, suction, cohesion, degree of saturation, and capillary force. These factors are discussed in an order reflecting their interrelationships and influence on each other:

1. Particle size and distribution:

Size distribution and particle distribution are fundamental properties that describe the range of soil particle sizes and their relative proportions. They significantly influence other soil properties such as permeability, porosity, and curve curvature (SWCC) [4].

- Grain size distribution: Affects the packing and porosity of the soil, influencing its mechanical properties like shear strength and compressibility.
- Particle distribution: Refers to the spatial arrangement of different grain sizes, impacting the soil's structural stability and hydraulic behavior.

The Effect of Grain Size Distribution and Compaction Moisture Content on the Shear resistance for soil that is partially saturated: To examine the impact of grain size distribution on shear strength, researchers tested silica sands with different fines contents using triaxial compression tests. When tested at their residual moisture level, the study found that soil samples compacted at their ideal moisture content had higher peak shear strength. Furthermore, when tested at ideal moisture level and compacted at residual moisture content, soils devoid of particles demonstrated higher shear strength.

This study shows that the shear strength of soil is strongly influenced by the distribution of particle sizes, particularly when the moisture content is changing. Better packing was seen in well-graded soils with a wide range of particle sizes, which increased interparticle friction and decreased void ratios to produce higher shear strength. The shear strength of uniformly graded soils, on the other hand, was often lower because to higher vacancy ratios and less efficient particle interlock.

The Chlef sand from a real-world used in the case study, analyzed in similar conditions, showed that natural sand with a diverse grain size distribution had improved shear strength properties. The well-graded Chlef sand exhibited higher shear strength compared to uniformly graded sands, highlighting the practical

implications of grain size distribution in geotechnical engineering projects.

The distribution of particles and grain sizes play a critical role in determining how partially saturated soils behave mechanically. The shear strength of soils can be greatly increased, resulting in more stable and dependable soil structures, by making sure that the particle size distribution is well-graded and by maximizing the compaction moisture content [5].

2. Particle shape:

Particle shape affects the soil's packing density and interparticle friction. Angular particles tend to interlock more, increasing shear strength, while rounded particles may pack more densely but with lower frictional resistance.

Particularly in partially saturated circumstances, when water-air interfaces and capillary forces greatly affect soil strength, particle form is essential in controlling the mechanical behavior of soils. A notable case study conducted by Sarker sheds light on the particle shape effect on shear strength, offering valuable insights into engineering practice. The paper conducted a comprehensive investigation focusing on the morphology impact of particle on shear strength. The study involved laboratory testing using soil specimens with different particle shapes, including angular and rounded particles [6].

Their findings corroborated the widely observed phenomenon that irregularly shaped particles, such as angular grains, tend to create interlocking arrangements within the soil matrix. This interlocking enhances the soil's shear strength by promoting greater resistance to shearing forces. In contrast, soils composed of rounded particles exhibited not high shear strength because of significant interparticle friction absence.

Furthermore, the study conducted slope stability analyses based on their laboratory findings to demonstrate the practical implications of particle shape on engineering design. They observed that slopes constructed with soils containing angular particles exhibited superior stability, particularly in regions subjected to fluctuating moisture conditions.

The case study underscores the significance of considering particle shape in geotechnical engineering practice, Engineers and designers can leverage these insights to optimize soil selection and ultimately stability enhancement the

performance of infrastructure projects in challenging soil conditions.

3. Particles packing:

Packing refers to how soil particles are arranged within a given volume. It is influenced by grain size distribution, particle shape, and compaction effort. Higher packing density typically results in higher shear strength due to better particle interlock and reduced void ratios [7].

4. Soil structure:

Soil structure denotes the arrangement of soil particles and the pore spaces between them. It is influenced by factors like packing, particle distribution, and the presence of cementing agents. Well-structured soils exhibit higher shear strength and stability.

Soil structure includes the particles arrangement, pores, and aggregates which considered an essential point to determine the mechanical behavior of soils, particularly at partially saturated conditions where water distribution and pore structure significantly influence shear strength. A noteworthy case study conducted offers valuable insights about soil structure effect on shear strength in high water quantity of soil soils, providing practical implications for geotechnical engineering practice [8].

The conducted comprehensive investigation focused on the relationship between soil structure and shear strength in partially saturated soils. The study involved laboratory testing using soil specimens with varying structural arrangements, ranging from well-graded to poorly-graded soils, under controlled moisture conditions.

Their findings revealed a direct correlation between soil structure and shear strength, with well-structured soils exhibiting higher shear strength compared to poorly structured counterparts. This difference in shear strength was attributed to the presence of strong interparticle bonds and cohesive forces within well-structured soils, which enhanced load-bearing capacity and stability. Furthermore, the influence of soil structure on pore characteristics and water distribution patterns was analyzed. Well-structured soils were found to possess more uniform pore networks with enhanced connectivity, facilitating efficient water distribution and retention even under partially saturated conditions. This phenomenon contributed

to maintaining higher effective stresses within the soil mass, thereby augmenting shear strength.

Importantly, the study highlighted the practical implications of soil structure in geotechnical engineering applications, particularly in slope stability analyses and foundation design. By considering the soil structure impact on shear strength, engineers can make informed decisions regarding soil stabilization techniques and construction methodologies to mitigate risks and optimize project outcomes. The case study underscores the significance of understanding soil structure effects on shear strength in partially saturated conditions, providing valuable guidance for soil mechanics and geotechnical engineering practices [8].

5. Effective stress:

Effective stress (σ') is the stress carried by the soil skeleton, defined as:

$$\sigma' = \sigma - u \tag{1.1}$$

In partially saturated soils, effective stress is affected by matric suction (difference between pore air and pore water pressures) [4].

In saturated soils, the water held in the pores and the effective stress of the soil grain at any given location within the soil mass share the same effective stress. The only particles of soil carrying the shear stress in a dry soil element are the grains themselves because there is no pore water pressure in dry soil so that the total stress and the effective stress are equal.

The effective stress in partially Saturated Soil, the presence of both air and water in the pores affects effective stress. The metric suction plays a significant role, as water content decreases, matric suction increases, leading to changes in effective stress.

The effective stress behavior of quasi-saturated compacted specimens of two distinct soil types (Gangetic silt and Canyon dam clay) was examined in this work. The goal of the study was to determine how the mechanical behavior of these quasi-saturated soils is affected by their initial condition, which is located on the recompression line in the water content (w) versus the natural logarithm of effective stress (ln(σ^')) space. The results of the investigation demonstrated that both soil types' shear strengths are highly impacted by effective stress. Consolidation results

from increased effective stress, which also lowers water content and increases shear strength. Because different soil types react differently to variations in effective stress, soil-specific research is crucial for precise geotechnical forecasts and designs. When designing and building slopes, foundations, and other geotechnical structures, knowledge of the effective stress behavior of quasi-saturated soils can help ensure stability and performance across a range of loading circumstances [9].

6. Suction:

Suction in soils includes osmotic and matric. Matric suction is the primary component in partially saturated soils, enhancing effective stress and shear strength. It can be expressed as [10]:

$$\text{Matric Suction} = u_a - u_w \quad (1.2)$$

(σ') effective stress is a key concept in soil mechanics, representing the stress borne by the soil skeleton. It is calculated as the difference between total stress (σ) and pore water pressure (u). In partially saturated soils, suction, or the differential between pore air and water pressure, further influences effective stress.. This factor can notably impact the soil's mechanical properties, especially its shear strength.

Wu et al. in 2022 investigated the effects of matric suction on the partially saturated clay shear strength reinforced with polypropylene fiber in 2022. Triaxial shear tests were performed on unsaturated clay samples that were reinforced with polypropylene fibers from the Shaoxing portion of the East Zhejiang Grand Canal as part of the investigation. Higher matric suction was observed to improve both the effective internal friction angle and the total cohesion intercept, suggesting greater resistance to shear deformation. However, the adsorption angle of internal friction decreased while matric suction increase, suggesting a diminishing contribution to shear strength at higher suction levels. Additionally, the study identified an optimal fiber length of 12 mm for significantly improving the soil's shear strength parameters. The stress-strain relationship was found to be approximately hyperbolic with strain-hardening characteristics, which became more pronounced with increasing matric suction, indicating more plastic behavior under higher suction. Volumetric strain sensitivity was notably higher compare to net confining pressure changes, increasing linearly when matric suction was zero [11].

In conclusion, Wu et al.'s study highlighted the crucial role of matric suction in enhancing the shear strength of unsaturated soils and demonstrated the beneficial effects of polypropylene fiber reinforcement. These findings emphasize the importance of considering both effective stress and matric suction in geotechnical engineering projects involving unsaturated soils [11].

7. Degree of saturation and capillary force:

The degree of saturation (S_r) is known as ratio of water to the of voids. It affects capillary forces, which arise due to surface tension at the air-water interface within soil pores. Higher degrees of saturation typically reduce capillary forces, lowering shear strength.

The findings an experimental Study on the Effects of Matric Suction [11]:

- When the saturation level reached roughly 50%, the cohesiveness and internal friction angle (two measures of shear strength) started to rise.
- Subsequent increases in saturation caused the shear strength to drop after this threshold.
- About 50% of saturation was the ideal level to maximize shear strength.
- Capillary cohesion was found to be responsible for the increased shear strength at moderate saturation levels; this cohesion was most effective up to the 50% saturation threshold.

8. Cohesion

As the component of shear strength Cohesion (c') attributed to intermolecular forces and cementation between soil particles. In partially saturated soils, apparent cohesion can also arise from capillary forces and matric suction.

Soil cohesion is a fundamental parameter in geotechnical engineering. It represents the shear strength attributed to intermolecular forces and cementation between soil particles. These cohesive forces arise due to attractive interactions at the particle level. When soil particles are closely packed, cohesive forces contribute significantly to shear resistance. In soil mechanics, cohesion is a critical component of the Mohr-Coulomb shear strength equation. The equation relates shear strength (τ) to normal stress (σ), cohesion (c'), and the angle of internal friction (ϕ):

$$\tau = c' + \sigma \tan \phi \qquad (1.3)$$

when normal stress is zero cohesion represents shear strength it accounts as soil particles attraction between each other. Cohesion particularly is significant in clay as cohesive soils where interparticle bonding is strong [12].

9. Angle of friction:

The internal friction angle (ϕ) is a significant metric used to describe the frictional strength of soil. It is primarily governed by the slipping friction between soil grains and the interlocking among them. The angle is altered by various Component such as shape of particles, packing of particles are, and the effective stress applied to the soil. Generally, a higher internal friction angle corresponds to a higher shear strength of the soil.

The angle of Internal Friction describes the resistance to sliding along a shear plane, It depends on the type of soil and particle arrangement, For cohesionless soils (such as sands), the angle of friction dominates shear strength.

In partially saturated soils, apparent cohesion can also arise from capillary forces. These forces result from tension of the surface at the air and water interface within soil pores. When water partially fills the voids, capillary forces contribute to apparent cohesion. As the degree of saturation increases, capillary forces diminish, affecting shear strength [12].

10. Shear strength:

Shear strength (τ) is soil's resistance indicator to shear stress and is influenced by effective stress, cohesion, internal friction angle, and matric suction. The shear strength of partially saturated soils can be expressed as:

$$\tau = c' + \sigma' \tan \phi' + S \tag{1.4}$$

c' is the effective cohesion, S represents the contribution of suction, and ϕ' is the internal friction angle [13].

In conclusion, the mechanical characteristics of partially saturated soils are interdependent, with each factor influencing and being influenced by others. Understanding these relationships is crucial for accurate modeling and prediction of soil behavior under various conditions. By examining these factors comprehensively, geotechnical engineers can better design and analyze soil structures to ensure stability and safety.

Shear resistance relation with a degree of saturation, variations in the silty sand's shear strength with saturation levels at Dr of 0%, 40%, 70%, and 90% for various vertical net stresses (50, 100, and 200)kPa. Note: The legend's numbers for relative density and vertical net stresses are arranged from left to right. Figure 1.2 shows a nonlinear trend in shear strength with a degree of saturation and an increase in shear strength with vertical stress [14].

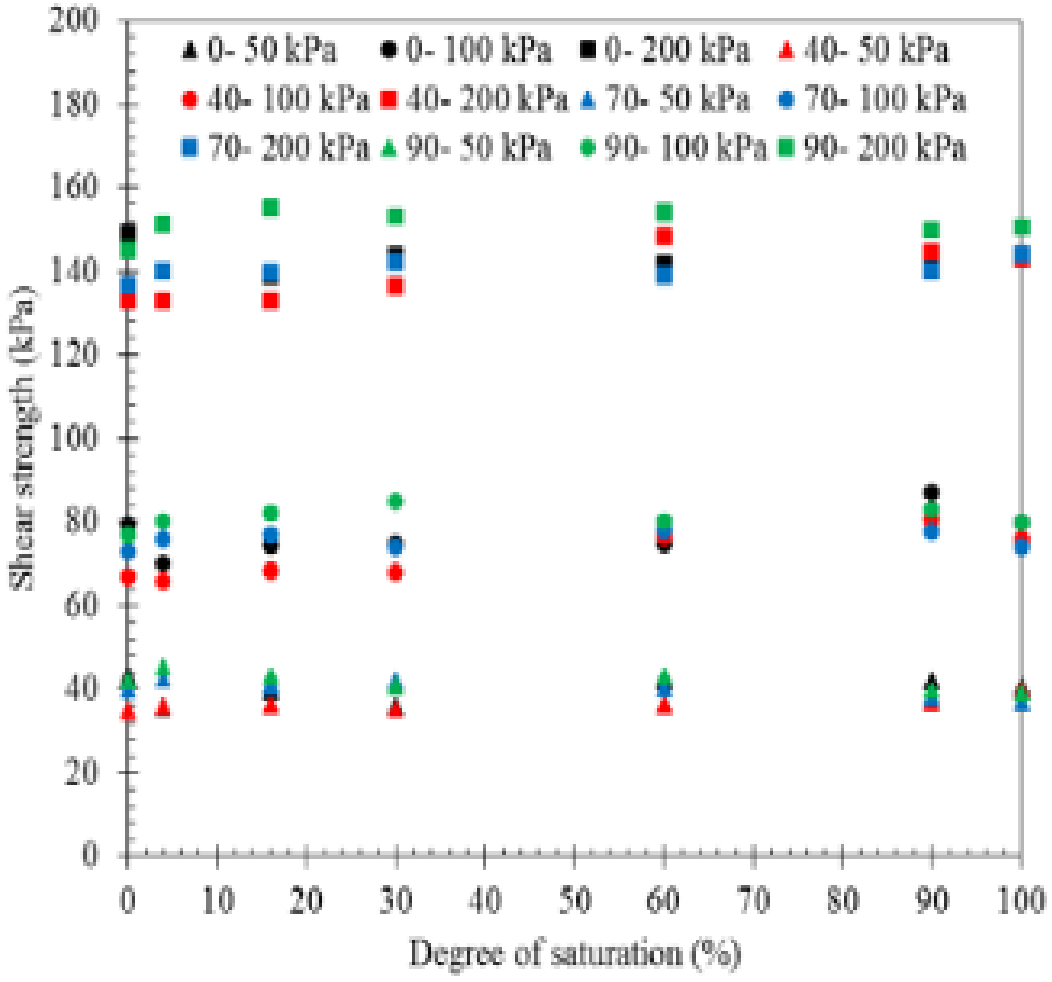

Figure 1.2 Silty sand's shear strength against the saturation rate [14].

The saturation rate and the suction impact the effective stress in unsaturated soils. Several models provide various formulas for figuring out the effective stress in unsaturated soils [15-19].

The following formula calculates the effective stress in unsaturated soils It was proposed by [20] :

$$\sigma' = (\sigma - u_a) - \sigma^s \quad (1.5)$$

σ′ known as total stress, σ known as suction stress, and u_a is the pore air pressure. For simplicity, the suction stress can be calculated as the product of matric suction and effective saturation. In the above case, the effective saturation from the SWRC (Soil Water Retention Curve) is used to measure the matric suction obtained from Equation (1.6) and, therefore, the following equation helps in finding the suction stress:

$$\sigma^s = -\frac{S_e}{\alpha}(S_e^{\frac{n}{1-n}} - 1)^{1/n} \quad (1.6)$$

The Mohr-Coulomb failure criterion for unsaturated specimens can be measured as shown below, the suction stress for the purpose of interpreting direct shear tests:

$$\tau_f = c' + \{(\sigma - u_a) + \sigma^s\}tan\varphi' \quad (1.7)$$

In this case, c' stands for the drained cohesion, which is typically taken to be zero for non-cemented soils, φ' for the drained internal friction angle, and τ_f for the shear stress at failure for a certain effective saturation. According to, this angle is independent of variations in matric suction or saturation levels and is generally equal to the friction angle obtained from direct shear experiments on saturated soils [21,22].

1.4 Failure Envelopes

The investegation of the silty sand under different saturation degrees shows the peak normal stress of different relative densities of (90%, 70%, 40%, and 0%) noted in (green, blue, red, and black) lines respectively [14].

This study shows that the initial relative density of soil significantly influences the Retention Curve (SWRC), shear strength, and effective stress in unsaturated soils. In denser soils, higher matric suction develops, which significantly enhances shear strength. Additionally, the findings reveal that both the degree of saturation and relative density influence the stress-displacement curve shape and the failure mode observed in the soil during shearing. An increase in the relative density of the unsaturated silty sand tested led to greater shear strength and suction stress. As relative density increased, the disparity in shear strength between saturated and unsaturated soils also grew, suggesting that models based on fully saturated soil conditions might be more conservative for denser soils.

Strength Characteristics Of Unsaturated Soils: Bishop introduced a widely

recognized equation for the shear strength of unsaturated soils, as illustrated below Terzaghi's principle of effective stress was extended for saturated soils. In this equation [15].

$$\tau = c' + [(\sigma - u_a) + \chi(u_a - u_w)]tan\phi \quad (1.8)$$

The term $(u_a - u_w)$ represents matric suction, with χ being a parameter dependent on the degree of saturation. χ varies from 1 to 0, reflecting conditions from fully saturated to completely dry. Bishop's equation is composed of two segments. The initial segment correlates to the shear strength of fully saturated soil, applicable when the pore-air pressure u_a , equals the pore-water pressure u_w. This part is influenced by normal stresses as the shear strength parameters c' and ϕ remain fixed for saturated soil. The latter segment accounts for the effect of matric suction, referred to as suction strength (τ_{us}).

The mechanical properties of unconsolidated soils are distinct from those of consolidated rocks, particularly in terms of varying saturation levels. For consolidated rocks, the frame moduli, Km and μm, are influenced by the properties of the solid grains (Ks and μs), the porosity (ϕ), and the degree of consolidation, as stated by Pride [23]. A straightforward method for estimating these moduli in consolidated rock involves measuring its response when dry, as noted by Mavko [24]. The frame moduli of consolidated rock, Km and μm, are unaffected by saturation levels since they primarily reflect the properties of the matrix. In contrast, unconsolidated soils show a high sensitivity to saturation (Sw), as their frame properties vary significantly. The addition of water in unconsolidated soils results in opposing pore water pressures from air and water in the pores, alongside the lithostatic overburden stress. Additionally, capillary tension enhances the cohesion among soil particles, an effect known as capillary suction, which can increase the shear strength of these soils, as discussed by Hornbaker and Lu [25,26]. Blight introduced an empirical method to incorporate these dynamics into Terzaghi's classic definition of effective stress, further developed in studies by [27-30].

$$\begin{aligned} P_e(S_w) &= \sigma(S_w) - p_a\,[1 - \mathcal{X}(S_w)] - p_w\mathcal{X}(S_w) \\ &= \sigma(S_w) - p_a + \mathcal{X}(S_w)p_c(S_w), \\ &= \sigma(S_w) - p_a + \sigma_s(S_w), \end{aligned} \quad (1.9)$$

where g = 9.806 ms^{-2} is the Earth's gravitational acceleration $\sigma = p_b(S_W)gz$ is the

overburden stress, and $p\zeta = \rho_j gz$, where ζ = w and a are the water and air pore fluid pressures, respectively. Keep in mind that the capillary pressure, which is shown by $p_c(S_w) = p_a - p_w$, is related to the saturation level using the proper constitutive models. Capillary suction stress is generally referred to as $\sigma_s = \chi(S_w)p_c(S_w)$. The integration of capillary effects into macroscopic behavior is made possible by the effective stress parameter, which is $0 < \chi(Sw) < 1$. This parameter depends on the local saturation of the soil [31] .

Numerous scholars propose that the effective saturation of the medium can be used to approximate it. This can be written as $\mathcal{X} = S_{we} = (S_w - S_{wr})/(1 - S_{wr})$, where S_{wr} represents the residual water saturation [32,33,34]. As a result, the Equation becomes equal to Terzaghi's famous effective stress relation for fully saturated media, $Pe = \sigma - p_w$, for totally water-saturated soil, where $\chi = 1$. As is typical when working with unconsolidated materials, it should be noted that the Biot-Willis coefficient is assumed to be close to unity [35].

1.5 Shear Strength of Different Degrees of Saturation

Bláhová presented data in Figure 1.3 and Table 1.1 that details how maximum shear strength (τmax), cohesion (c), and friction angle (ϕ) vary with different water contents in soil. The study found that the maximum shear strength at 10% water content was slightly greater than at 9% and significantly higher than at 11% water content. The friction angle was observed to be lowest at 11% water content (7.47°) and highest at 10% water content (13.4°), with a measurement of 9° at 9% water content. Additionally, as water content increased, cohesion consistently decreased [36].

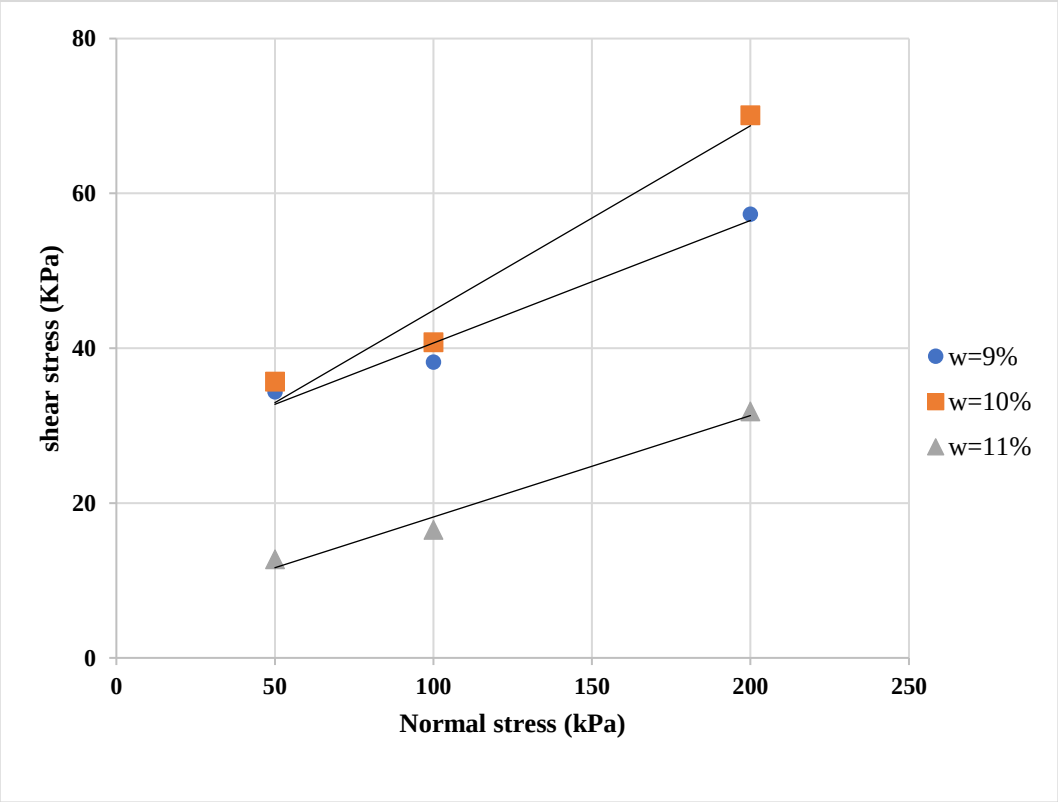

Figure 1.3 Mohor circle for different methods [36].

Table 1.1 Average prediction errors and shear parameter [36].

Water content	c(kPa)	φ(°)	τ_{max} 50kN	τ_{max} 100kN	τ_{max} 200kN
9%	24.84	9,00	34.39	38.22	57.32
10%	21.00	13,40	35.7	40.8	70.1
11%	5.09	7,47	12.74	16.56	31.85

1.6 Undrained Direct Simple Shear Testing Methods of Soils

There are a few methods to calculate the shear strength for partially saturated soil, but the Modified direct shear method is the most recommended due to its controllable environment with a small modification, it can present the closest case to reality, the method used in this study is often referred to as "sealed case" approach. This method involves hermetically sealing the soil sample to maintain a specific humidity level, thereby accurately simulating field conditions. By

controlling environmental factors within the test setup, the sealed case method allows for precise measurements of soil behavior under varying degrees of saturation. This controlled setup is particularly useful for replicating real-world conditions and observing the changes in shear strength as the soil transitions from dry to wet states. The results garnered from this testing provide invaluable data for designing and improving geotechnical projects, ensuring that they are safer and more resilient to environmental changes. This method's adaptability and accuracy make it a preferred choice among engineers who require reliable data for critical decision-making in soil stability analysis.

Undrained direct simple shear test for consolidated cohesive soils: Cohesive soil sample is placed between two rigid, parallel plates, with constraints applied both axially and laterally to maintain a constant cross-sectional area during this procedure. After axial loading, the sample is permitted to solidify in one dimension. The rate of axial displacement indicates that extra pore water pressures have mostly dissipated, at which point each increment of the normal load is regulated. One cycle of secondary compression is accomplished while maintaining the maximal normal load., or for an additional day after excess pore water pressure has ceased. Subsequently, the sample is subjected to shearing using a shear strength apparatus. During the shearing process, the volume of the specimen is kept constant to simulate undrained conditions. This is accomplished by adjusting the applied normal load to ensure the specimen’s height remains unchanged. Since there is no pore pressure during shearing, changes in normal stress are considered equivalent to changes in effective stress and are assumed to match the changes in pore water pressure that would occur in a sealed specimen under constant total stress. The shear strength is assessed under constant volume conditions, replicating undrained conditions for a saturated specimen. This test is therefore relevant to field conditions where soils have fully consolidated under a specific set of stresses and are then subjected to stress changes without sufficient time for additional drainage to occur.

Under the constant volume (undrained) strength, the relationship with stress conditions is crucial. This testing method assesses the strength under conditions of plane strain, where the principal stresses undergo continuous rotation due to applied shear stress. Such a simple shear stress condition mirrors many real-world scenarios, including zones below extensive embankments and around piles

subjected to axial loading. This method helps in understanding the material's behavior in practical situations where stress conditions are dynamic and complex. The stress state within the simple shear specimen lacks adequate definition and uniformity, which hampers a rigorous interpretation of the results. While presenting the data in terms of shear stress and normal effective stress on the horizontal plane is beneficial for engineering applications, it's important not to mistake these for the effective stress parameters derived from other shear tests with more clearly defined stress states. The secant shear modulus values can serve as a basis for estimating the initial settlements of embankments constructed on saturated cohesive soils, arising from undrained shear deformations [37] specific designation D6528-07.

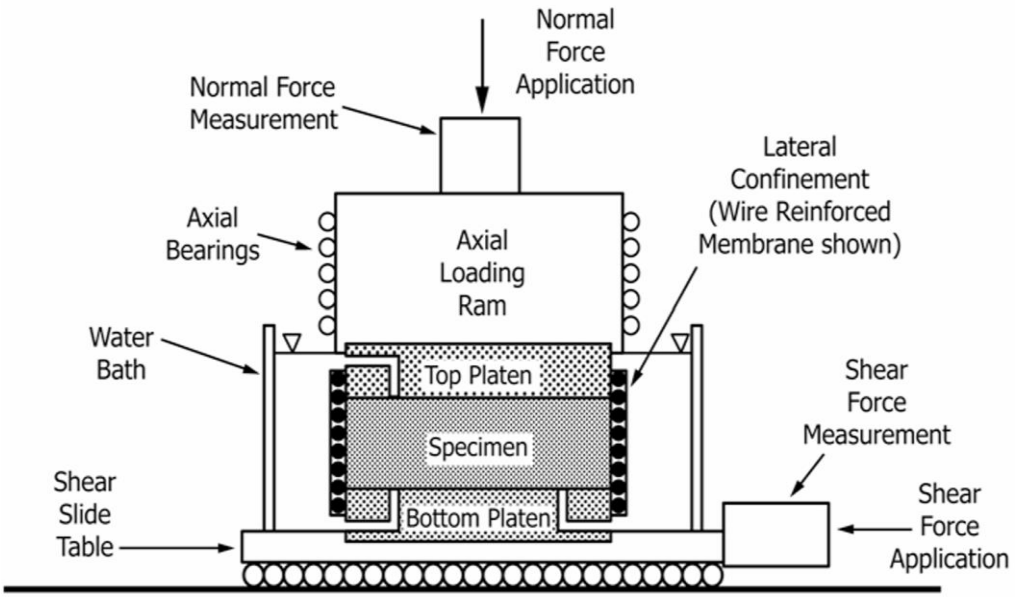

Figure 1.4 Schematic Diagram of Essential Direct Simple Shear Components [37].

Figure 1.4 provides a visual representation of the essential components required for the apparatus. Further sections will outline the specific criteria and specifications for each of these components. The lateral confinement device must ensure that the specimen remains laterally constrained, with the cross-sectional area not changing by more than 0.1% during shear. Moreover, the confinement must facilitate uniform shear deformation. Circular specimens are typically confined using a wire-reinforced membrane or stacked rigid rings, while square specimens are confined using stacked hollow plates or hinged solid plates. The thickness of the individual stacked rings or plates should be less than 1/10 of the specimen thickness to enable

relatively uniform shear deformation. If the confining device is placed within a water bath, it must be constructed from corrosion-resistant materials. [37].

The specimen size requirement should be as follows; the minimum diameter (or lateral dimension) of the specimen should be 45 mm, and the minimum height should be 12 mm. Additionally, the ratio of height to diameter, or the minimum lateral dimension, should not exceed 0.4. The specimen height should be at least ten times the maximum particle diameter. For the top and bottom platens of the apparatus they must be made of corrosion-resistant material and shaped in a circular, rectangular, or square cross-section to match the specimen. They should be designed to firmly hold the porous disks in place, facilitate drainage from the specimen to the water bath, and transfer shear to the specimen without any horizontal slippage. The porous disks used should be made of materials like brass, silicon carbide, aluminum oxide, or similar rigid and corrosion-resistant substances. These disks need to be flat, with a fine texture to prevent soil intrusion into the pores, yet rough enough to effectively transfer shear stress. They must possess permeability at least ten times greater than that of the soil. Covering at least 90% of the specimen surface, if smaller than the specimen, they should be recessed into the platen to ensure the surface in contact with the soil is flush with the platen. The water bath serves to offer the specimen unrestricted access to water at atmospheric pressure, thus preventing specimen drying from evaporation. One approach involves submerging the entire specimen and confinement device in a water bath, while another involves connecting the end platens to a standpipe via flexible tubing. In both scenarios, water needs to be accessible to both ends of the specimen through the porous disks. All the previous equipment and devices along with the usual direct shear devices and apparatus will be needed to prepare the sample.

Sample preparation starts after the sampling of the soil specimen is complete, Efforts should be made to minimize soil disturbance caused by vibration, distortion, and compression. Compact the material in batches, layer by layer, using either a pressing or kneading action into a preparation mold or directly into the cutting shoe. Before adding material for the next layer, scarify the top of each layer. When compacting soil directly into the cutting shoe, create the specimen in at least three layers, ensuring that the compacted material is thicker than the final trimmed specimen. Utilize the specimen setup frame to insert the fully trimmed specimen

into the confinement device. The cross-sectional area (A) of the specimen may be considered as that of the confinement device or the cutting shoe [37].

The explained procedure and standards above were the difference points between the standard direct shear test and the undrained shear test, and after all these differences are controlled, the normal direct shear reading is taken while the direct shear box is water-submerged in the direct shear apparatus, making sure the no water is leaking from the apparatus.

1.7 Controlling the Saturation Degree of Soil

Partially saturated sand affects the stability of foundations for buildings and mega-structures significantly. For instance, while fully saturated loose sands are subjected to cyclic loads like earthquakes, and liquefaction during seismic activities, they can lose their strength and act like a liquid. This can cause significant settling and tilting of structures. However, partially saturated sands, which have gas bubbles, demonstrate different properties and can help reduce the risk of liquefaction.

Researchers have performed experiments using shaking tables on shallow foundations built on partially saturated sands. These sand samples were created by mixing denture cleanser powder, which contains hydrogen peroxide, with dry sand at various saturation levels (from 79.5% to 98%). The findings indicated that both the settlements and the excess pore pressures were less in partially saturated sand models compared to those nearly saturated. Notably, the decrease in settlement was more significant at lower saturation levels, lower relative densities, and higher stress conditions. The generation of gas bubbles through chemical means seems to be an effective strategy for minimizing settlements caused by liquefaction in shallow foundations during seismic events [38].

Engineers need to account for the degree of saturation when designing foundations on sandy soils. Employing innovative methods, such as creating partial saturation with chemical agents, can enhance the performance of foundations and increase seismic resilience. In essence, comprehending how partially saturated sand impacts the stability of building foundations is essential for maintaining safety and stability during seismic activities [38].

Treating partially saturated soil to withstand shear testing involves careful preparation to ensure accurate and reliable results. Here's a comprehensive

explanation:

1. Understanding Partially Saturated Soil: Partially saturated soil contains both water and air in its pore spaces. This condition affects the soil's behavior and strength characteristics, making it crucial to address before conducting shear tests.
2. Saturation Control: The first step in treating partially saturated soil is to control its saturation level. This can be achieved by subjecting the soil sample to a specific moisture conditioning process. The goal is to reach a consistent degree of saturation throughout the sample, ensuring uniformity in test results.
3. Equilibrium Saturation: It's essential to attain equilibrium saturation, where the soil sample reaches a stable moisture content. This ensures that the soil's properties remain constant throughout the testing process, minimizing the changes in the content of water on shear strength.
4. Sample Preparation: Once the soil reaches equilibrium saturation, it's prepared for shear testing. This involves carefully compacting the soil into the desired shape and dimensions while maintaining its saturation level. Special attention should be paid to avoiding air entrapment and ensuring uniform compaction.
5. Confinement and Drainage: During shear testing, the partially saturated soil sample must be properly confined to simulate field conditions accurately. Confinement devices should be designed to allow for drainage and prevent pore pressure buildup during shearing. This ensures that the soil's response to shear loading is accurately captured.
6. Moisture Monitoring: Throughout the shear testing process, it's important to monitor the moisture content of the soil sample to ensure consistency. Changes in moisture content can significantly impact shear strength, so maintaining a stable moisture condition is crucial for reliable test results.
7. Data Interpretation: Finally, the results of the shear tests on partially saturated soil should be carefully interpreted considering the soil's moisture condition. Understanding how saturation levels influence shear strength allows engineers to make informed decisions regarding soil stability and behavior in real-world applications.

By following these guidelines, engineers can conduct shear tests on partially saturated soil samples with confidence, leading to more accurate assessments of soil behavior and stability [39].

Enhancing the strength of foundations in saturated sand is essential for ensuring the stability and durability of structures. Several techniques are effectively employed to achieve this: Dynamic Compaction involves the repeated dropping of a heavy weight on the soil surface, which is particularly effective in permeable, granular soils and helps reduce settlements, seismic subsidence, and liquefaction potential. For organic soils, dynamic compaction can be used to create sand or stone columns. Another method, Vibro Compaction, compacts granular soils by rearranging soil particles into a denser state through vibratory probes, thus improving soil density and bearing capacity [39].

One of the most effective but lesser-used methods is the use of geosynthetic-reinforced soil foundations, which involve reinforcing the soil with geosynthetics such as geogrids to enhance bearing capacity and reduce footing settlement. This technique has been widely applied in treating soft soil foundations. Additionally, proper sand integration is essential, involving the use of appropriate concrete and mortar mix ratios and thorough compaction of sand during backfilling to meet the specified density according to relevant building codes, which include mandated testing, usage guidelines, and construction methods. Selecting the appropriate soil improvement technique depends on soil conditions, cost-effectiveness, and long-term performance, making consultation with experienced geotechnical engineers essential for successful implementation [40].

1.8 Importance of Image Analysis

Image analysis has emerged as a critical tool for evaluating the shear strength of soil, a key factor in geotechnical engineering that determines the stability and safety of structures such as buildings, bridges, and dams. Unlike traditional methods, which rely on manual measurements and can be subjective and error-prone, image analysis provides a more accurate and objective assessment by using high-resolution imaging to capture the detailed properties of soil samples. This technique enables precise characterization of microstructural features, like particle size, shape, and arrangement, which are crucial for understanding soil behavior under

shear stress. Additionally, image analysis streamlines data collection and processing through automation, enhancing efficiency and consistency while reducing the time and effort needed for soil testing. Modern imaging technology also allows for real-time monitoring of soil conditions during shear tests, offering immediate feedback that is vital for prompt decision-making in construction and engineering projects. Non-destructive testing methods, such as digital image correlation, further enable repeated analysis of the same soil sample under varying conditions without causing damage, preserving the sample for ongoing study. Integrating the detailed data from image analysis with numerical models allows engineers to simulate soil behavior more accurately, improving predictive modeling and enabling the design of safer, more effective structures. Thus, image analysis greatly improves the understanding, efficiency, and precision of assessing soil shear strength, ultimately enhancing the safety and reliability of construction projects. Detailed Insights into Soil Microstructure that image analysis provides [39,40]:

- Visualization: Image analysis allows for high-resolution visualization of soil particles and their arrangements, providing clear insights into the soil's microstructure.
- Particle Shape and Size: Detailed measurements of particle shape, size, and distribution can be obtained, which are crucial for understanding soil behavior.
- Deformation mechanisms: like tracking changes which enables tracking of soil deformation over time, offering a dynamic view of how soil structures change under stress.
- Failure Mechanisms: Identifies and visualizes failure mechanisms, such as shear bands and crack formations, which are difficult to observe with traditional methods.
- Quantitative data: for Precision it Provides precise quantitative data on soil displacement and strain, improving the accuracy of soil behavior models. For parameter analysis it assists in determining critical parameters like porosity, density, and void ratio, which are essential for predicting soil performance under various conditions.
- Non-destructive testing: it works as preservation where Image analysis is non-destructive, allowing for repeated observations of the same sample

without altering its properties.

- Real-time Monitoring: Facilitates real-time monitoring of soil behavior during experiments, enhancing the understanding of immediate responses to loading.
- Applications: in research and development where it is Widely used in research to develop new soil models and to validate theoretical predictions. For engineering practice it also Helps in practical applications such as foundation design, slope stability analysis, and assessing the effectiveness of soil improvement techniques.

Image analysis is a valuable tool in geotechnical engineering, offering detailed, accurate, and real-time insights into the mechanical behavior of soils. Its ability to visualize and quantify soil microstructure and deformation mechanisms significantly enhances both research and practical applications in soil mechanics.

A model utilizing Vision Transformer (ViT): Measuring the sample's shear resistance is the main objective of the test. Shear strength is important when constructing stable and secure structures like slopes, retaining walls, and foundations. It plays a major role in explaining the importance of accurately predicting soil shear strength in geotechnical engineering applications. Traditional methods often involve manual testing, which can be labor-intensive and time-consuming. using computer vision techniques to automate this process, specifically utilizing ViT models. The proposed methodology involves collecting images of transparent soil samples, where shear strength is indicated by the deformation patterns within the soil. These images are then processed and fed into a Vision Transformer model for regression, where the model learns to predict shear strength values directly from the images. The [41] paper outlines the experimental setup of the experiment, including details on data collection, preprocessing steps, model architecture, and training procedure. Various performance metrics are discussed to evaluate the effectiveness of the proposed approach. It presents the performance of the ViT-based regression model compared to baseline methods and traditional regression techniques. The authors demonstrate that their approach achieves superior accuracy in predicting shear strength values from image data.

Previous studies have explored various image analysis techniques for soil characterization, including particle size distribution analysis, pore structure

quantification, and soil deformation tracking. These methods have been applied to a wide range of soil types and engineering scenarios, demonstrating their effectiveness in capturing intricate soil features and behavior.

However, despite these advancements, challenges remain in accurately predicting key geotechnical parameters, such as shear strength, from soil images. Traditional regression models may struggle to extract meaningful relationships between image features and soil properties, particularly in complex and heterogeneous soil systems. In this context, the work by Wang J. represents a significant advancement in the field by proposing a Vision Transformer based image regression model. By leveraging the power of deep learning and attention mechanisms, the ViT model learns to directly map image representations to shear strength values, bypassing the need for manual feature engineering or intermediate feature extraction steps. This novel approach not only streamlines the process of soil characterization but also holds promise for enhancing the accuracy and efficiency of geotechnical engineering analyses. The integration of ViT models into soil mechanics research opens up new avenues for advancing our understanding of soil behavior and improving predictive models for engineering design and risk assessment. It underscores the transformative potential of deep learning techniques in automating complex tasks and accelerating innovation in soil science and engineering practice [41].

Cement-filled, translucent soil is used for the research. To create the transparent cemented soil samples, a pore solution with a matching refractive index, fused silica, and nanoscale hydrophobic fumed silica powder was utilized. The fumed silica powder served as a binding agent when combined with refractive-index-matched fused quartz sand. The fumed silica powder, which dries to a white powder, was mixed with four various-sized quartz sand particle sizes (0.1–0.2 mm to 1.0–3.0 mm) with a density of 2300 kg/m³. The mixture that resulted from testing various pore fluid ratios was measured for refractive index using an Abbe refractometer. With the highest transparency and a refractive index of 1.4585 at 25°C, the mixture of n-dodecane and 15# white mixed mineral oil at a mass ratio of 1:20 was found [41].

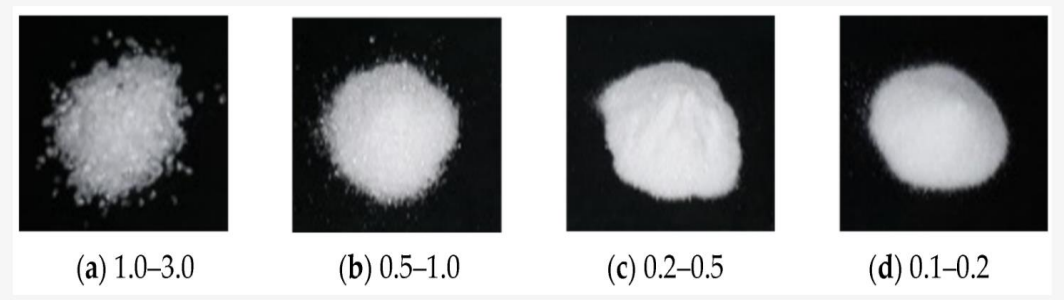

Figure 1.5 Fused Quartz sand [41].

Figure 1.5 shows the preparation phase for the transparent dirt specimen process. (a) Cleaning the samples using water to remove impurities, followed by oven drying. (a) Mixing n-dodecane and number 15 white oil to create the pore solution till the refractive index reaches 1.4585. (c) Accurately measuring and combining the generated pore solution, silica powder, and blended quartz sand. ensuring that there is adequate mixing to enable the silica powder to stick to the quartz sand particles' surfaces. The air addition gave the material a transparent or milky white appearance. (d) Compacting the translucent cement-filled soil and packing it into a 150 mm long by 25 mm wide test tube. The test tube's gas was removed after 30 minutes in a vacuum chamber, enabling the soil particles to rearrange under air pressure and achieve a 70% compaction level [41].

Cemented Transparent soil composition:

- Transparent cemented soil patches composed of fused quartz sand were used in the investigation.
- As shown in the picture below, four distinct quartz sands were chosen, each with a particular grain size: fine (0.1–0.2) sand, medium (0.2–0.5) sand, coarse (0.5–1) sand, and fine gravel (1-3).
- For every size of quartz sand particle, varied amounts of fumed silica powder (from 0% to 20%) were added.

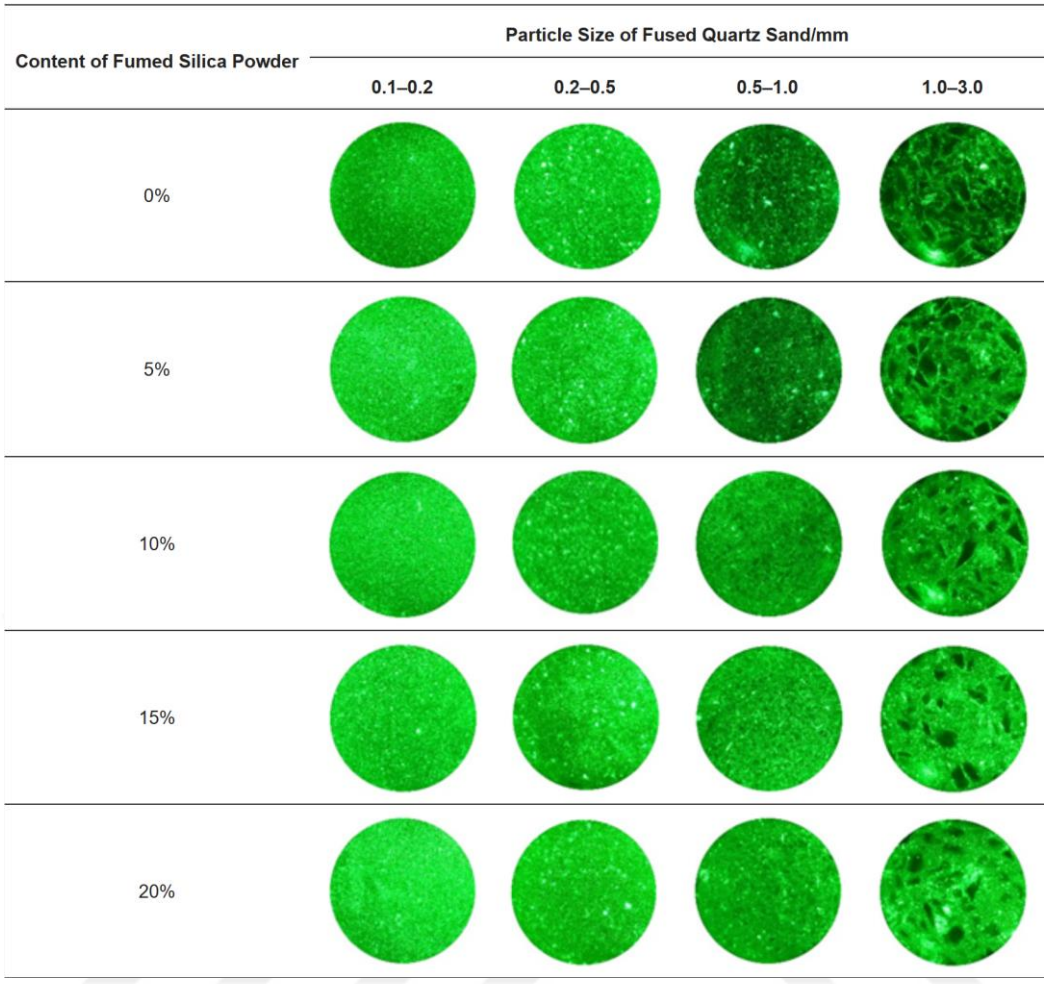

Figure 1.6 Transparent soil's speckle image [41].

Scatter collection test shown in Figure 1.6, To demonstrate the better performance of the suggested feature extraction model (backbone network component) on this dataset, state-of-the-art backbone networks are used as a comparison. The prediction error, which is the difference between expected and actual values, is the evaluation metric. Histograms representing the statistical data are shown with a normal fit curve. VGG and ResNet, two well-known backbone networks with a track record of effectiveness in image classification and regression under a variety of conditions, are the networks under comparison. The University of Oxford researchers created the VGG network, a deep convolutional neural network distinguished by its notably deep architecture and usage of relatively small convolutional kernels (usually 3 × 3). Fewer parameters can be used by the VGG network thanks to this approach. ResNet uses shortcut connections spanning multiple layers to solve the gradient problem. By directly passing input data (i.e., intermediate characteristics) down several layers to the next one, these shortcut

connections let the neural network optimize residual data more successfully. ResNet can effectively train deep networks without experiencing performance deterioration because of this method. Table 1.2 provides an overview of the average prediction errors and training timeframes for the various approaches [41].

Table 1.2 Training durations and typical prediction errors for various techniques [41].

Method	Training duration	Average cohesion Error	Average angle of friction error
ViT	**124 min**	**1.64**	**0.73**
Resnet	**78 min**	**3.95**	**2.33**
VGG	**55 min**	**5.27**	**2.26**

By modifying the fumed silica content and the fused quartz sand particle size, transparent-soil samples with different parameters were created in order to verify the effectiveness of the suggested method. Direct-shear tests were used to measure the shear strength and cohesiveness of the resulting transparent cemented soil with various amounts. These soil samples were then subjected to controlled laser spot capture, producing two transparent soil datasets. Based on test results, the following deductions were made [41]:

By contrasting it with traditional ResNet and VGG models, the efficacy of the suggested feature extraction module was shown. Findings from both datasets showed that the CNN + ViT feature extraction module performed better in forecasting transparent soil shear strength. Higher prediction accuracy and a narrower error distribution were demonstrated by this approach.

To make predictions, fifty samples were selected at random, and the correlation coefficients between the true and predicted values were calculated. The findings validated the excellent dependability of the approach with correlation coefficients of 0.93 and 0.94 in the two datasets [41].

Examining how fractal dimension affects sand-geosynthetic interface shear resistance. The study employed a variety of materials, including different sands (ND1 River Sand, NK1 Rounded Sand, NK3 Crushed Stone), geomembranes, EPS Geofoam, a digital microscope, and image processing software (Fiji-ImageJ). The sands were evaluated based on their shape, roundness, and surface roughness, with the grains being rounded and analyzed using image processing techniques. Several types of geomembranes with different roughness levels were used, along with EPS Geofoam of three distinct densities. The geomembrane surfaces were examined with a digital microscope to determine their fractal dimensions. The methodology involved processing sand images, assessing the roundness and fractal dimensions of the grains, examining the surface structure of geosynthetics, and calculating the fractal dimensions of geomembrane surfaces. Direct shear box tests were conducted to explore the shear resistance of various sand-geosynthetic interfaces, with the goal of understanding the impact of grain shape, geosynthetic surface roughness, and hardness on shear resistance [42].

Grain images were captured using a camera with a 21-megapixel resolution, which was mounted on a fixed setup 20 cm above the ground. The grains were placed on a non-reflective black cloth for imaging. The geomembranes used in the research measured 10x10 cm, with their tensile behavior evaluated according to ASTM D 638/D6693 standards. A digital microscope was utilized to examine the surface structure of the geomembranes and obtain profiles for fractal dimension analysis. Fiji-ImageJ, an open-source image processing software was used for image processing purposes. Fiji aims to offer a version of ImageJ equipped with numerous plugins. Written in Java, ImageJ software remains open source, facilitating ongoing evolution and interdisciplinary collaborations. Access to the latest software versions is available through the website 'https://fiji.sc/'.

Modifications were made to the shear box apparatus to conduct tests on geosynthetic-soil interfaces. Following ASTM D 5321 guidelines, the geosynthetics were affixed to a rigid surface for testing purposes. To achieve this, wooden slats with a height of 2.5 cm were prepared to match the dimensions of the shear box chamber. Instead of using slats of uniform width, slats with varying widths but consistent height were chosen for the test setup. This arrangement allowed the geosynthetic to utilize the compression devices of the shear box

chamber in the shear direction, preventing displacement and ensuring uniform attachment to the rigid surface. The objective was to establish a continuous interface between the geosynthetic and the soil throughout the shear process, eliminating the need for area leveling [42].

The research focused on estimating the fractal dimensions of both sand and geosynthetic materials, examining their impact on interface shear resistance. Image processing methods were employed to determine area-perimeter values of sand particles, allowing for the estimation of their fractal dimensions. Additionally, surface profiles of geomembranes were captured using a digital microscope for further analysis [42].

Table 1.3 Classification of soil groups based on roundness values and Fractal Size [42].

Soil	Roundness	Fractal Size (D_R)	Class	Average angle of friction(degree)
ND1	**0.8332**	**1.0311**	**Fully rounded**	**38**
NK2	**0.7644**	**1.1591**	**Semi-rounded**	**43**
NK3	**0.6927**	**1.2663**	**Angular**	**49**

Shear box experiments were carried out at a relative density (Dr) of 50%. The sand was placed in accordance with ASTM D 3080 standards and sheared at a rate of 0.5 mm/min under normal stress levels of 54.5 kPa, 109 kPa, and 163 kPa until reaching a 10% strain. It was noted that an increase in the fractal dimension of the particles led to higher internal friction angles. The maximum internal friction angle, reaching 49°, was observed for NK3 sand with a fractal dimension of 1.2663, whereas the minimum angle, at 38°, was recorded for ND1 sand with a fractal dimension of 1.0311 more details shown in Table 1.3 [42].

This research explored how particle shape, geosynthetic surface roughness, and stiffness influence interface shear resistance through fractal theory. It observed that the fractal dimensions accurately depicted the shape of sand particles and the

roughness of geomembrane surfaces. Additionally, it noted a correlation where higher fractal dimensions of sand particles corresponded to increased internal friction angles. Higher fractal dimensions of materials correlated with increased interface friction angles, with the roughest geomembrane surfaces requiring more displacement for interface mobilization. In EPS geofoam interfaces, higher density (stiffness) resulted in lower friction angles, with particles of greater fractal dimensions penetrating the surfaces more significantly. Overall, reduced stiffness and increased roughness of geosynthetic surfaces improved interface efficiency. The study's findings highlight the successful quantification of these effects through fractal dimensions, though further verification with large-scale tests is recommended [42].

1.9 Direct Shear Test

The Direct Shear Test is a fundamental laboratory procedure used in geotechnical engineering to determine the shear strength of soil materials. It provides valuable insights into soil behavior, stability, and the interaction between particles. This section will explore the direct shear test method, its relevance to soil mechanics, and how it can be adapted for studying partially saturated sand.

Measuring the sample's shear strength is the main objective of the test. Shear strength is important when constructing stable and secure structures like slopes, retaining walls, and foundations.

1.9.1 Apparatus

The test apparatus consists of a shear box (usually circular or square-shaped) with two metallic plates. Two porous stones, screws, a gripper disk, and a loading cap are also part of the setup. The shear box restricts horizontal strain but allows shearing along a horizontal plane. The soil sample should be placed in the shear box. Initially, a direct normal pressure (consolidation stage) is applied to the top of the sample. The metallic plates are screwed together during consolidation. The shearing stage begins by applying a shearing stress along a pre-determined horizontal plane. The shearing device maintains a constant displacement rate to ensure accurate results. During shearing, the applied shear stress and corresponding horizontal displacement are recorded. The test continues until the specimen fails (usually along a shear plane), after finding more than two peak shear values under

different normal stress Mohr-Coulomb (M-C) Failure is drawn, and through the Mohr-Coulomb and the previously explained calculation the angle of friction and cohesion are identified that can be used in the calculation that can show the bearing capacity of the soil used in the procedure [43].

1.9.2 Relevance to Soil Mechanics

- Foundation Design: Direct shear test results inform foundation design by providing shear strength parameters. Engineers use these parameters to calculate bearing capacity and assess stability.
- Slope Stability Analysis: Understanding shear strength is crucial for slope stability assessments. The direct shear test helps predict soil behavior during earthquakes and other geotechnical events.
- Soil Behavior Modeling: Shear strength data from direct shear tests contribute to soil behavior models. These models aid in numerical simulations and geotechnical analyses.

Adaptation for partially saturated sand; Capillary Effects: In partially saturated soils (such as partially saturated sand), capillary forces play a role. Apparent cohesion arises from capillary forces due to surface tension at the air-water interface within soil pores. Test Modifications: To adapt the direct shear test for partially saturated sand; Control the water content to achieve the desired degree of saturation. Consider capillary effects when interpreting cohesion and shear strength.

1.10 Dilatancy

In soil mechanics, dilatancy refers to the volume change observed in granular materials subjected to shear deformation. Unlike many solid materials, compacted dense granular materials tend to expand in volume when sheared. This occurs because the grains in a compacted state interlock, restricting their movement relative to each other. When stress is applied, a lever motion between neighboring grains causes the material to bulk expand. Conversely, a granular material in a very loose state may continuously compact rather than dilate under shear. A material is described as dilative if its volume increases with shear, and contractive if its volume decreases with shear.

The phenomenon of dilatancy can be observed during a drained simple shear test on a sample of dense sand. Initially, as the shear strain increases, the volumetric

strain decreases, causing the soil sample to compact. As the stress approaches its peak value, the volumetric strain begins to increase. With further shearing, the soil sample ends up with a larger volume than at the start of the test. The extent of dilation is strongly influenced by the initial density of the soil, with denser soils exhibiting greater volume expansion under shear. Additionally, the angle of internal friction decreases as the effective normal stress is reduced.

Dilatancy is crucial in geotechnical engineering due to its significant impact on soil behavior under shear stress. It influences the angle of internal friction, which measures the soil's shear strength. As confining pressure increases, the angle of internal friction rises until it reaches a peak value, indicating maximum shear strength. Beyond this peak, the angle of internal friction decreases abruptly, signifying a reduction in shear strength. This behavior is essential for designing stable structures like slopes, footings, tunnels, and piles. Engineers must account for the potential decrease in strength post-peak to ensure the long-term stability and integrity of these constructions. Understanding dilatancy allows for better prediction and mitigation of soil deformation and failure, leading to safer and more effective geotechnical designs.

In this seminal work, Bolton investigates the behavior of sands under different conditions, focusing on strength, dilatancy, and their interplay. Bolton compiles extensive data on the strength and dilatancy of 17 grains of sand subjected to either axisymmetric or plane strain conditions. These sands were tested at various densities and confining pressures [44].

Critical state angle of shearing resistance:

- Mineralogy is the primary factor influencing the critical state angle of soil shearing resistance during shearing at constant volume.
- The angle of shearing resistance can be experimentally determined within a margin of about 33° for quartz and 40° for feldspar.
- The concept of critical state soil mechanics plays a central role in understanding soil behavior.

Correlation between dilatancy and shearing behavior:

- Bolton correlates the extra angle of shearing observed in “dense” soil with its rate of dilation.

- The denser the soil, the greater its tendency to dilate during shearing.
- The relative density and mean effective stress are combined into a new relative dilatancy index.

The Dilatancy angle is defined as follows:

$$tan\psi = \frac{\Delta V}{V} \tag{1.10}$$

Where: ΔV represents the change in volume during shearing, V is the initial volume of the soil sample, [44] introduced a method to estimate the maximal dilatancy angle for well-compacted granular soils, proposing that under triaxial conditions, the angle (ψ) can be expressed as $3.75\times I_R$ and under plane strain conditions expressed as $6.25\times I_R$, where I_R represents the relative dilatancy index. This index I_R can be determined for well-compacted granular soils using the formula:

$$I_R = 5 \times D_r - 1 \quad (0 < I_R < 4) \tag{1.11}$$

$$D_r = \frac{(e_{max} - e)}{(e_{max} - e_{min})} \tag{1.12}$$

For cohesive soil, dilatancy behavior differs. Bolton suggests that in laboratory tests, normally consolidated clays may show no dilatancy. Consequently, for cohesive soils, dilatancy is assumed to be dependent on the preconsolidation state. The maximal dilatancy angle (ψ) for cohesive soils is proposed as:

$\psi = 0°$ for normal or light-over consolidated soils

$\psi = \phi'/6$ for overconsolidated soils

$\psi = \phi'/3$ for heavily overconsolidated soils

Several practical implications for geotechnical engineering. One key point is the preference for using secant strength values over tangent strength values, as suggested by Bolton, to better reflect soil behavior. The rate of dilatancy, influenced by both effective stress and soil density, significantly impacts soil behavior and must be considered in engineering designs. Additionally, the paper's proposed correlations have important implications for both laboratory and field-testing procedures, aiding in more accurate assessments of soil properties [44].

However, despite advances in understanding soil behavior, a gap remains between research findings and engineering practice. Engineers often face challenges in effectively applying these research insights to practical design scenarios,

highlighting the need for continued efforts to bridge this divide.

1.11 Aim of the Study

During this study the focus was on a variety of saturation of high percentages, to identify the most critical saturation degree. The study aims to grasp the behaviors of sand and to supply the knowledge to be used for predicting the behavior of sand in the field under loads with the experimented range of the degree of saturation since there are conditions of partial saturation sandy soils in reality, it is interesting to be able to determine or predict the shear strength of the soil to reach the stability of the superstructures, furthermore how different water content is linked to the normal stress and the effect of different water content on the volume change due to the different interaction of water molecules on the particles of sand and how they compress and dilate, although the study isn't on the microscopical scale, but image analysis is a useful tool for feature extraction that can help in pattern recognition.

1.12 Hypothesis

In order to determine the relationship between mechanical behavior and saturation rate, this study aims to measure the shear strength of several similar remolded samples with varying saturation levels between 0 and 100 degrees on a 5%-degree interval. Each sample encountered a direct shear test with controlled normal stresses of 62.5, 125, and 250 kPa, and each of these normal stresses was repeated 3 times for accuracy. This area is of interest to the geotechnical field mainly because the soil serves as the primary foundation for superstructures and foundations and maintaining the stability of the soil is crucial to extending the life of these structures. Additionally, because all soils undergo a process of saturation and evaporation that affects their bearing capacity, studying sand can help reflect the behavior change that occurs in most soils. Volume changes because of interactions between soil and water particles result in expansion and dilatation. A customized direct shear box was constructed close to field state while preventing water leakage from the sample.

2
MATERIAL USED AND METHODOLOGY

The experimental work carried out in this project investigated the effect of a high degree of saturation on the shear strength parameters and volume change of unsaturated sand using direct shear tests. This chapter details the materials, apparatus, and sample preparation techniques used. Additionally, the testing schedule, including the number of tests conducted and the types of normal stresses applied, is presented.

2.1 Material Proprieties

2.1.1 Soil Type

Two different D_r of the same sand were used in the experiment they are labeled as (SS1) for (**35%)** and (SS2) for (**65%**), as shown in Figure 2.1. The required experimental procedure was made to obtain the preliminary physical parameters for these sands, its summarized in Table 2.1, From the test results it has been concluded that the material used was poorly graded loose (SS1) and medium dense Sand (SS2).

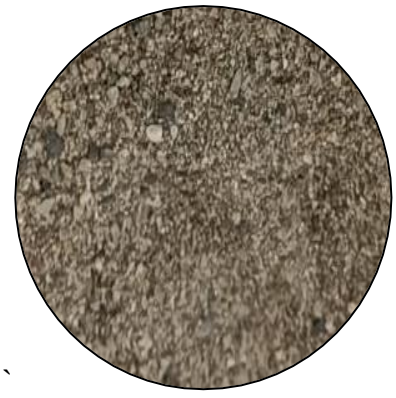

Figure 2.1 Sand sample.

Table 2.1 Geotechnical properties of the sand

Characteristics	**SS1**	**SS2**
Soil classification	**SP**	
Specific Gravity, G_s	**2.68**	**2.68**
Dry unit weight, γ_{dry} (kN/m^3)	**15.38**	**16.40**
Saturated unit weight, γ_{sat} (kN/m^3)	**19.45**	**20.09**
Natural void ratio, e_o	**0.71**	**0.60**
Minimum void ratio, e_{min}	**0.47**	
Maximum void ratio, e_{max}	**0.83**	
Relative density D_r %	**35**	**65**
Porosity n	**0.41**	**0.36**
D_{10}	**0.58**	
D_{30}	**0.31**	
D_{60}	**0.13**	
Coefficient of curvature Cc	**1.27**	
Coefficient of uniformity, Cu	**4.46**	

The grain size distribution curves of these samples were obtained using sieve analysis as shown in Figure 2.2.

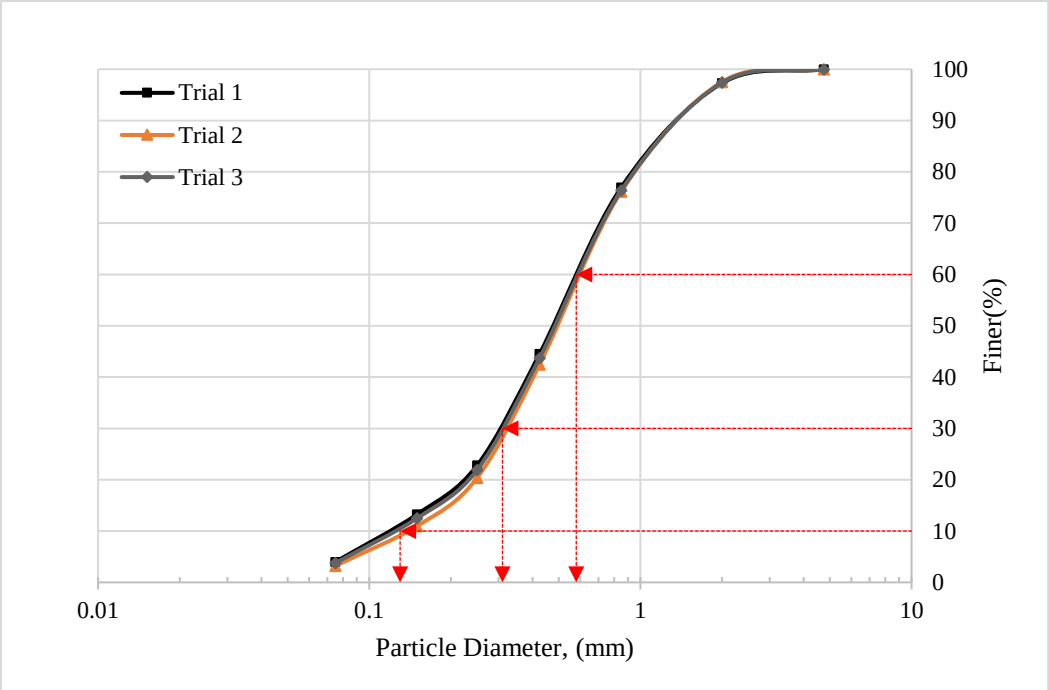

Figure 2.2 Sieve analysis graph.

2.1.2 Silicon Grease

Silicone grease, also known as dielectric grease or silicone compound, is a lubricant made from silicone oil and a thickener, usually a silica-based substance. It is commonly used for its water-resistant and non-reactive properties. It's composed of Silicone Oil, which is the primary component, usually polydimethylsiloxane (PDMS), which gives the grease its slippery and water-resistant characteristics. Thickener Often silica or a similar compound, which thickens the oil to a grease-like consistency. Silicon grease holds great properties;

- Water resistance: Highly resistant to water, making it ideal for use in wet or underwater environments.
- Temperature stability: Maintains its properties over a wide temperature range, typically from -40°C to 200°C (-40°F to 392°F).
- Non-conductive: Acts as an electrical insulator, preventing electrical connections from shorting out.
- Non-Corrosive: Does not corrode metals or other materials, making it safe for use on a variety of surfaces.
- Chemical stability: Resistant to oxidation and chemical breakdown, ensuring long-lasting performance.

Silicon grease is effective as a sealing agent along with its water resistance and none friction behavior make it ideal to seal the gaps in the shear box to offer the partially saturated soil a fully undisturbed environment because it binds with the walls of the shear box yet it doesn't have any effect on the sliding layers and its water phobic behavior makes it impenetrable by water.

2.2 Experimental Procedure

2.2.1 Sieve Analysis

A sieve analysis was conducted to determine the particle size distribution of the sand tested in this study. The sieves used (#4, #8, #16, #30, #40, #50, #100, #200) are shown in Figure 2.3. The sieves were weighed along with the oven-dried sand sample (500 grams) to be used in the test. The sand was then poured into the sieves and placed in the shaker for ten minutes. After shaking, each sieve, along with the residue retained, was weighed. The collected data were plotted, as shown in Figure 2.2, and the values for D60, D30, D10, Cu, and Cc were calculated and presented in Table 2.1.

Figure 2.3 Sieve analysis apparatus

2.2.2 Relative Density (Minimum and Maximum Voids Ratio)

Relative density, also known as the density index, is a measure that compares the difference between the void ratios of cohesionless soil in its loosest state and its densest state to the difference between the void ratios in the loosest state and the soil's current natural state.

$$Relative\ Density = \frac{e_{max} - e_{nat}}{e_{max} - e_{min}} \quad (2.1)$$

Where,

e_{max}= The void ratio of the loosest state for coarse-grained soil.

e_{min}= The void ratio of the densest state for coarse-grained soil.

e_{nat}= The void ratio of the natural field state for coarse-grained soil.

the porosity of soil is affected by the grain shape, the uniformity of grain size, and the conditions under which the soil was deposited. As a result, porosity alone does not indicate whether the soil is in a loose or dense state. To ascertain this, the porosity or void ratio of the given soil must be compared to the porosity or void ratio of the same soil in its loosest and densest possible states. This comparison leads to the concept of relative density.

$$Relative\ Density = \frac{e_{max} - e_{nat}}{e_{max} - e_{min}} \quad (2.2)$$

$$e = {V_v}/{V_s}; \quad (2.3)$$

V_v: Volume of voids

V_s: Volume of solid

$$\gamma_d = {S.G * \gamma_w}/{(1 + e)} \quad (2.4)$$

$S.G$: Specific gravity,

γ_w: Unit weight of water,

e: Voids ratio

$$e = {S.G * \gamma_w}/{\gamma_d} - 1 \quad (2.5)$$

$so, e\ is\ inversely\ proporational\ to\ its\ dry\ density(\gamma_d)$

$$Relative\ Density = \frac{\frac{1}{(\gamma_d)_{min}} - \frac{1}{(\gamma_d)}}{\frac{1}{(\gamma_d)_{min}} - \frac{1}{(\gamma_d)_{max}}} \quad (2.6)$$

Relative density is an arbitrary characteristic of sandy deposits. It represents the ratio of the actual reduction in the volume of voids in sandy soil to the maximum possible reduction in void volume, indicating how much more the sand can be compacted beyond its natural state. Determining relative density is useful for compacting coarse-grained soils and evaluating the safe bearing capacity of sandy soils. For very dense gravelly sand, a relative density greater than one can be achieved, suggesting that such dense natural packing cannot be replicated in a laboratory setting.

Procedure Calibration of the mold:

1. Use a Vernier caliper to measure the inside diameter of the mold at various depths and determine the average value.
2. Position the mold on a flat surface or plate, measure its height at multiple locations, and compute the average (accuracy = 0.025 mm).
3. Calculate the volume of the mold.
4. Fill the mold with distilled water until it overflows.
5. Weigh the water that fills the mold.
6. Record the water temperature.
7. Refer to physical tables to find the density of water at the recorded temperature.
8. Calculate the mold's volume by dividing the weight of the water by its density.
9. Confirm the mold's volume by using the weight of the water divided by the water's density.
10. Dry the soil sample in an electrically controlled oven.
11. Cool the sample in a desiccator.
12. Separate soil lumps without breaking the individual particles.
13. Sieve it through the required sieve size.

For Maximum density: First, weigh the empty mold (W). Then, attach the collar to the top of the mold and secure it with a clamp. Fill the mold with the oven-dried soil sample until it reaches halfway or two-thirds of the collar's height. Secure the mold onto the vibrating deck using nuts and bolts, and place the surcharge weight

on top. Run the vibrator for 8 minutes. Finally, weigh the mold with the soil and record the weight (W2).

$$mass\ of\ dry\ soil\ M_s = (W_2 - W_1)gm \tag{2.7}$$

$$(\gamma_d)_{max} = {M_s}/{V\frac{g}{cc}} \tag{2.8}$$

$$e_{min} = (S.G * \gamma_d)\ /\ (\gamma_d)_{max}\ - 1 \tag{2.9}$$

Maximum void ratio (Minimum Density): The procedure begins with accurately weighing the empty mold (W). Dry, pulverized soil is then poured into the mold using a funnel, ensuring a steady stream. The spout is adjusted to maintain a consistent free fall of 25 mm for the soil particles, using a spiral motion from the rim to the center. This process continues until the soil fills the mold to approximately 25 mm above the top. The soil is then leveled off, and the weight is recorded (W1).

Separately, 1 kg of sand is carefully poured into a graduated cylinder, which is then covered with Teflon to prevent disturbance. The cylinder is inverted ten times to mix the sand. Measurements of height and diameter are taken to assess volume change. This process is repeated for ten trials to determine the maximum void ratio.

$$mass\ of\ dry\ soil\ M_s = (W_1 - W_2)gm \tag{2.10}$$

$$(\gamma_d)_{min} = {M_s}/{V\frac{g}{cc}} \tag{2.11}$$

$$e_{max} = (S.G * \gamma_d)\ /\ (\gamma_d)_{min}\ - 1 \tag{2.12}$$

Natural density: Obtain a representative soil sample for the test. Make sure the sample is prepared in accordance with standardized procedures, measure the weight of the mold containing dry soil. With the volume of the mold known, you can compute the natural density, γdry, of the dry soil.

$$e = {(S.G * \gamma_w)}/{\gamma_d}\ - 1 \tag{2.13}$$

$$Relative\ Density = \frac{e_{max} - e_{nat}}{e_{max} - e_{min}} \tag{2.14}$$

2.3 Modified Direct Shear Test

2.3.1 Direct Shear Test

The goal of this test is to evaluate the shear strength of soil using the direct shear apparatus. These parameters, specifically the angle of internal friction and cohesion, are crucial in engineering projects like foundation design, retaining walls, slab bridges, pipes, and sheet piling. The direct shear test provides a quick method to estimate these values. This laboratory report details the procedures for determining these parameters specifically in cohesionless soils, below are the apparatus required to proceed with the procedure

1. Direct shear box apparatus.
2. Loading frame with attached motor.
3. Transducers (for measuring various parameters).
4. Proving ring (for measuring shear force).
5. Tamper (for compacting soil).
6. Straight edge (for leveling soil surface).
7. Balance (capacity up to 200 grams).
8. Spatula (for handling soil samples).
9. Porous stone (to facilitate drainage).
10. Pan (for collecting drained water).
11. Oven (for drying soil samples).
12. Additional balance (for weighing soil samples and other materials).
13. Knife (for trimming soil samples).
14. Silicon grease (for lubricating shear box components).
15. Tape (for sealing containers and securing instruments).
16. Screwdriver (for assembly and adjustments).
17. Funnel (for controlled pouring of soil).
18. 30 cm pipe (possibly for preparing samples or for drainage).

Strain-controlled direct shear machine includes several components: a shear box, a soil container, a loading unit, a proving ring, and transducers for monitoring shear deformation and volume changes. The shear box typically consists of two circular pieces that enclose the soil sample. The soil container is where the soil sample is placed for testing, and the loading unit applies normal stress or load onto the soil. The proving ring measures the shear load that is applied to the soil along the plane

of shearing. Transducers are used to monitor and record both shear deformation (displacement) and volume changes within the soil sample during testing. These components collectively facilitate precise measurement and analysis of shear strength properties of soils under controlled conditions.

Procedure:

1. Check the internal dimensions of the soil container for accuracy.
2. Assemble the soil container according to specifications.
3. Calculate the container's volume and weigh it to establish its mass.
4. Fill the container with soil in uniform layers around 10 mm thick; compact if necessary for a denser sample.
5. Weigh the filled container to determine the soil weight by subtracting the container's mass and calculate the soil density.
6. Level the soil surface carefully.
7. Place the upper grating and loading block on the soil surface.
8. Measure the thickness of the soil sample.
9. Apply the intended normal load.
10. Remove the shear pin to initiate shear testing.
11. Attach transducers to monitor any volume changes.
12. Record initial transducer readings and calibration values using computer software.
13. Verify all settings to ensure no connection exists between components except through the soil.
14. Activate the motor and record shear force data continuously.
15. Monitor and record volume change readings until failure occurs.
16. Connect all transducers to computer software for real-time data recording.
17. Utilize appropriate software to analyze and graph the collected data.

General notes:

- In shear box testing, the specimen fails along a predetermined or induced horizontal plane rather than its weakest plane. This limitation prevents the evaluation of stress states during loading, and failure occurs progressively.
- The direct shear test is simpler and quicker, utilizing thinner

specimens to enhance drainage of pore water. It also facilitates the study of friction between materials in the upper and lower halves of the shear box.

- The angle of shearing resistance in sands varies depending on factors such as compaction, grain size, shape, and surface roughness. It typically ranges from 28 degrees (very loose, round grains) to 46 degrees (dense, angular grains).
- Volume changes in sandy soils during shearing are influenced by factors including particle gradation, shape, and stress conditions. Loose sands tend to expand, while dense sands contract. The critical void ratio plays a significant role in governing this behavior.
- Friction between sand particles results from mechanisms such as sliding, rolling, and interlocking.
- The ultimate shear parameter values for loose and dense sands are similar, hence minor disturbances during sampling and specimen preparation have negligible effects on the calculation of the friction angle at the ultimate stage.

2.3.2 Direct Shear Apparatus

The direct shear apparatus is a laboratory device used to measure the shear strength properties of soil or other materials shown in Figure 2.4. It is a fundamental tool in geotechnical engineering for understanding the behavior of soil under shear stress. The components of the Direct Shear Apparatus are a shear box, oil container, loading unit, proving ring, 3 transducers (horizontal deformation transducer, shear deformation transducer, and volume change transducer), motor and drive system, and data acquisition system.

Figure 2.4 Direct shear apparatus.

Working principle

1. Sample preparation: The soil sample is placed in the shear box, with careful attention to achieve a uniform and representative sample.
2. Applying normal load: A normal load is applied to the sample using the loading unit. This load simulates the weight of the soil or structure above the sample in the field.
3. Shearing the sample: The motor and drive system apply a horizontal force to the upper half of the shear box, causing it to move relative to the lower half. This movement simulates the shear stress applied to the soil in the field with a speed of 0.5 mm/min.
4. Measuring responses: As the shear force is applied, the proving ring measures the shear load, and the transducers measure the horizontal displacement and volume changes. These measurements are recorded by the data acquisition system.
5. Data analysis: The recorded data are used to generate shear stress vs. shear

strain curves and to calculate the soil's shear strength parameters, such as the internal friction angle and cohesion.

2.3.3 Modified Direct Shear Box Preparation

The shear box used had a cylindrical internal shape with a diameter of 6.32cm and a height of 3.42cm. The gaps between the two halves of the shear box were sealed by a layer of silicon grease along the small drain holes and the bottom drain gap was sealed with grease and tape. To make sure there is no leakage from the gap, the box was filled with water and left for 24 hours in a controlled condition in the lap. There were no losses in water observed from the sample as the water was at the top of the box in Figure 2.5.

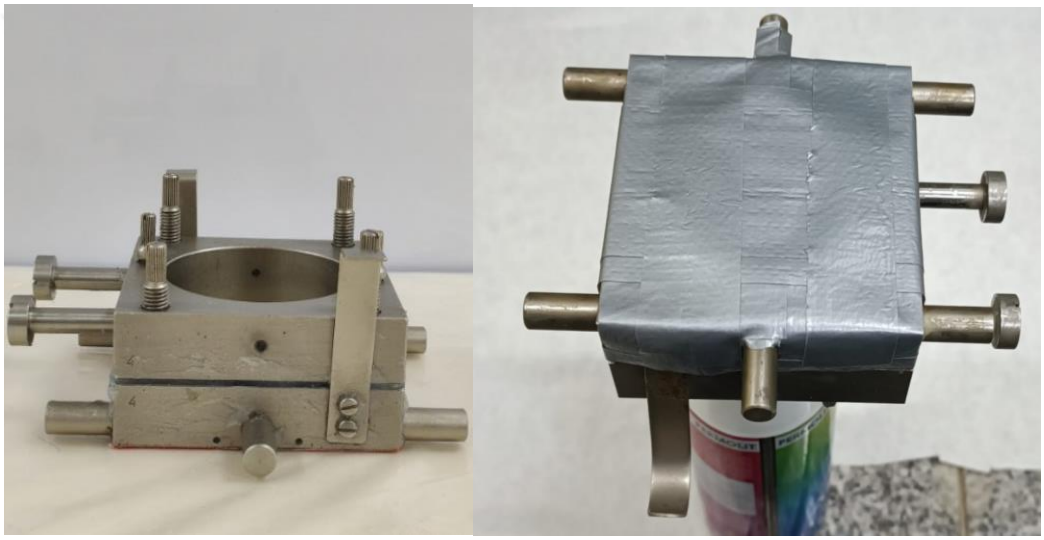

Figure 2.5 Modified direct shear box.

2.3.4 Modification Efficiency Check

In order to ensure that silicon grease doesn’t have any effect on the readings, a test was run only for the shear box containing only water while the gaps were sealed with grease as explained above and the results showed no shear resistance which means silicon grease didn’t cause friction or attraction between the shear box layers, the graph shown in Figure 2.6 proves it.

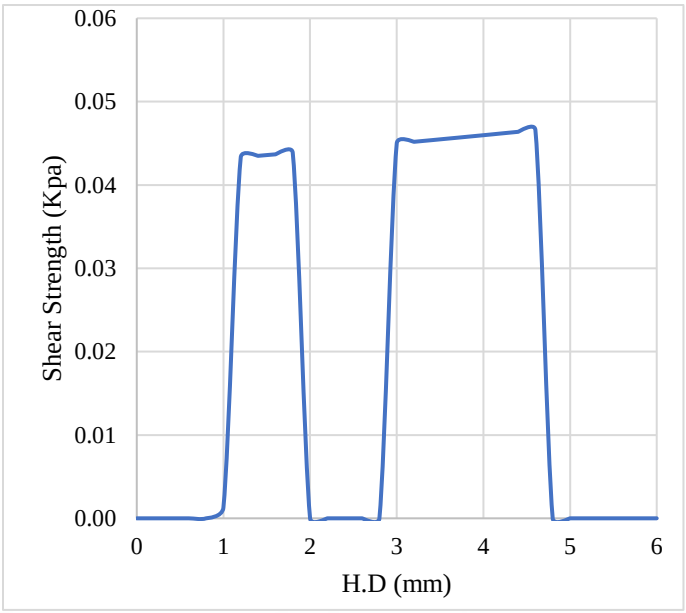

Figure 2.6 Efficient test.

2.3.5 Sample Preparation

The dry unit weight sample was prepared using the (Dry pluviation technique) as shown in Figure 2.7. In this method, the direct shear box was used as the sample container during the preparation and curing procedure, and trials involved placing oven-dried sand into the box using a funnel and circular motion starting from a zero-height surface.

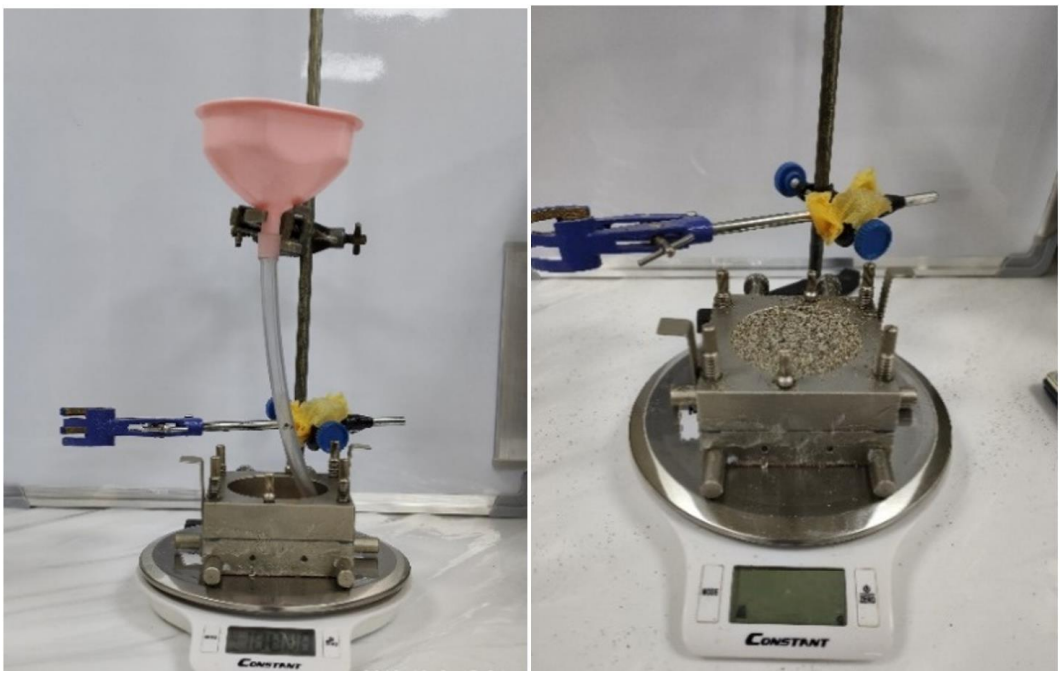

Figure 2.7 Dry Pluviation technique.

To create a fully saturated sample, the water pluviation technique was used as well with oven-dried sand (168.3g) for SS1 and (179.6g) for SS2. Here's how it was done:

1. Pour the sand into the box using a funnel.
2. Add the necessary amount of water (44.5 g) for SS1 and (40.4 g) for SS2 to saturate the sand in 3 equal levels so as not to disturb the soil as shown in Figure 2.8 below.
3. The resulting void ratio for SS1 and SS2 was 0.709 and 0.602 respectively.

Figure 2.8 Wet sample preparation.

2.3.6 Preparing Partially Saturated

To create a partially saturated sample, similar techniques as for the fully saturated sample were used. However, in this case, the sample was initially prepared fully saturated and then allowed to dry over a few days to control its saturation based on temperature until it reached the required saturation level. The saturation level is monitored by tracking the weight of the shear box as shown in the equation (2.17).

$$S\,e = G_s\omega \tag{2.15}$$

$$S = \frac{G_s\frac{m_w}{m_s}}{e} \tag{2.16}$$

$$m_w = m_{total} - m_{box} - m_s \tag{2.17}$$

Void ratio (e) is constant with controlled pouring techniques, G_s is constant and ω is observed via tracking the change in weight of the sample as explained above.

When the sample in the shear box reaches the required water content, it should be placed in a sealed bag or a container that is not affected by temperature change and not exposed to air to achieve an even distribution of water in the soil this phase is called the curing phase.

Identifying the exact duration needed for the curing phase took multiple tests with different durations from 1 hour up to a week, for each duration test the shear strength was compared with the previous duration until the duration of 24 hours observed that any more hours would not affect the shear strength, meaning that a 7-week curing duration would give similar results as the 24 hours, more details shown in Table 2.2 below, and it also was compared with [14] where the paper clarified to reach the moist equilibrium it should be left in airtight bag for 24 hours.

Table 2.2 Curing duration checkups (125kPa).

Trial	Duration (h)	Force reading	Peak Shear Strength(kPa)	Critical force reading	Critical shear strength(kPa)
1	**0**	**0**	**0.03**	**-**	**0**
2	**0**	**0**	**0.04**	**-**	**0**
3	**1**	**189.00**	**84.29**	**187.50**	**83.63**
4	**2**	**188.00**	**83.85**	**186.00**	**82.96**
5	**4**	**185.00**	**82.51**	**182.75**	**81.51**
6	**8**	**183.50**	**81.84**	**181.25**	**80.84**
7	**12**	**182.00**	**81.17**	**180.25**	**80.39**

Table 2.2 Curing duration checkups (125kPa). (continued…).

Trial	Duration (h)	Force reading	Peak Shear Strength	Critical force reading	Critical shear strength(kPa)
8	**24**	**181.25**	**80.84**	**197.25**	**87.97**
9	**48**	**181.20**	**80.82**	**179.00**	**79.83**
10	**96**	**181.10**	**80.77**	**179.10**	**79.88**
11	**168**	**181.20**	**80.82**	**179.00**	**79.83**
12	**600**	**181.25**	**80.84**	**179.10**	**79.88**

2.4. Image Analysis

In recent research, scientists have explored the impact of sand particle characteristics on soil shear strength. They've investigated factors like particle shape, size, and gradation. Irregularly shaped particles, such as angular ones, tend to enhance shear strength compared to spherical particles. Additionally, coarser, and well-graded sands exhibit improved shear behavior. These findings contribute to our understanding of soil mechanics and geotechnical engineering. These are the methods and uses:

1. Integrated Digital Image Analyses for Understanding the Particle Shape Effects on Sand–Geomembrane Interface Shear [45]:
   - Investigates the influence of particle shape on sand–geomembrane interfaces using X-ray micro-computed tomography (μCT).
   - Extract shape parameters (sphericity, roundness, fractal dimension) from sand specimens.
   - Conducts interface shear tests and analyzes micro-topographical changes after shearing.
   - Correlates irregular particle shapes with increased shear strength.
2. Influence of Particle Size on the Friction and Interfacial Shear Strength of

Sands [46]:

- Explores the effect of particle size on shear strength through direct shear and interface direct shear tests.
- Complemented by image analyses and surface roughness studies.

3. Evaluating the Influence of Sand Particle Morphology on Shear Strength [47]:

- Investigates particle shape, size, and gradation in sandy soil.
- Angular-shaped particles enhance shear strength compared to spherical ones.
- Coarser and well-graded particles also improve shear strength.

The method used was based on the studies [42], Here's a summarized version of the image processing steps performed in ImageJ software for particle analysis:

1. Load the image into the software.
2. Set the scale using a ruler.
3. Duplicate the image.
4. Convert the image to 8-bit grayscale.
5. Enhance contrast and separate particles from the background.
6. Apply the "Threshold" operation to create a binary format.
7. Fill gaps on particle surfaces using the "Close" command.
8. Eliminate particles with uncertain boundaries.
9. Perform particle analysis using the "Analyze Particles" command.

The Image analysis was performed after separating the particles to close sizes using sieves to put them in categories that can be captured by the camera to avoid distortion, the picture was taken in a dark room and light was in a cube shape box that had only the top part made of glass that allowed light to go through and the sand particles were distributed in even intervals on top of the glass, the light helped in clearly showing the particles size of the particles as shown in Figures 2.9 and 2.10 where each photo shows different size particles of (4.75-2)mm and (2-0.85)mm respectively.

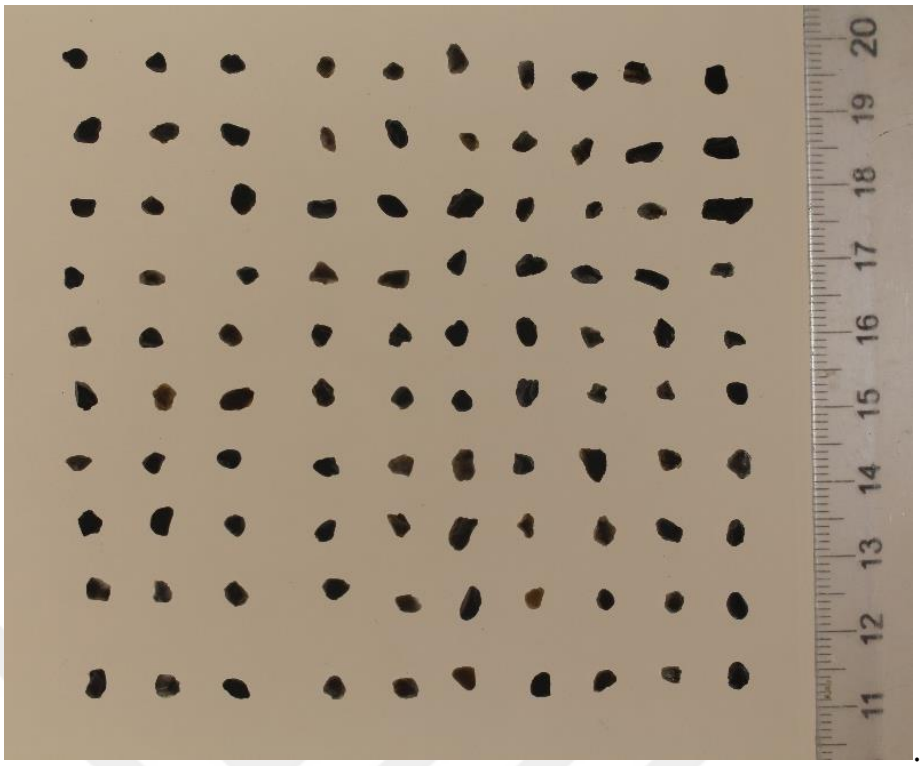

Figure 2.9 Original photo of the particles (4.75-2) mm before the image analysis.

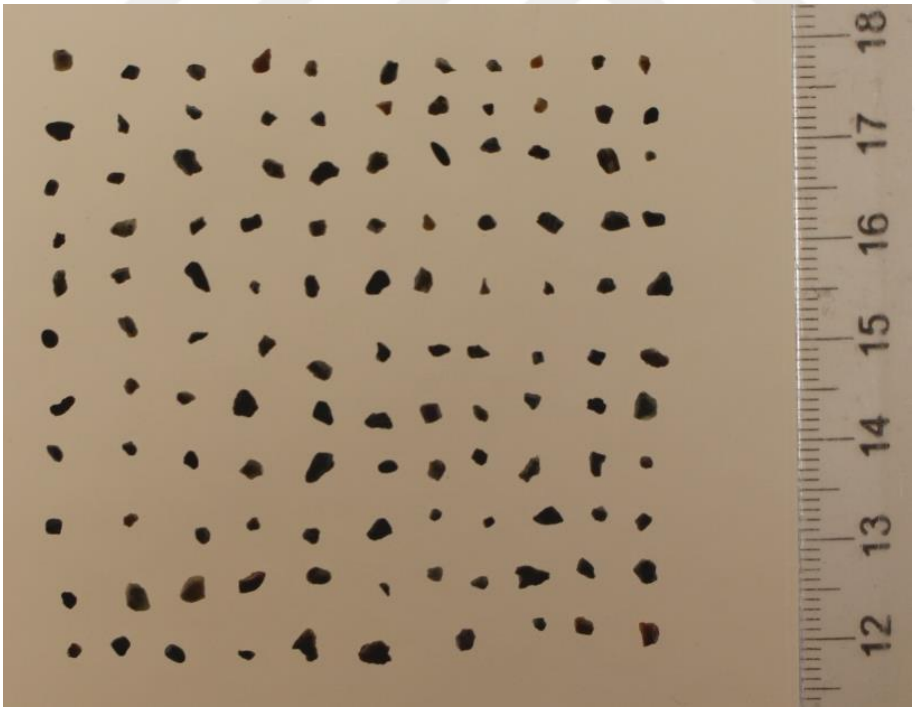

Figure 2.10 Original photo of the particles (2-0.85) mm before the image analysis.

3
TEST PREPARED

The test results and the highlights of the most important and interesting findings will be discussed in this chapter. The comparison between direct shear tests for dry, partially saturated, and saturated samples will be discussed. The shear strength increase, dilation, and sudden losses of strength are observed in unsaturated samples due to the occurrence of the common phenomenon will be observed, Along with Comparison with a different relative densities and the difference in dilation, lastly, the soil image analysis will be discussed the kind of shape the soil has.

3.1 Direct Shear Tests Prepared

Table 3.1 Test prepared.

	Relative density	Degree of saturation	Applied load (σ) kPa			Trial repeat
1	**35% (SS1)**	**Fully saturated (100%)**	**62.5**	**125**	**250**	**3**
2		**95%**				**3**
3		**90%**				**3**
4		**85%**				**3**
5		**80%**				**3**
6		**75%**				**3**

Table 3.1 Test prepared. (continued…)

	Relative density	Degree of saturation	Applied load (σ) kPa			Trial repeat
7	**35% (SS1)**	**70%**	**62.5**	**125**	**250**	**3**
8		**50%**				**3**
9		**25%**				**3**
10		**DRY (0%)**				**3**
11	**65% (SS2)**	**Fully saturated (100%)**	**62.5**	**125**	**250**	**2**
12		**95%**				**2**
13		**90%**				**2**
14		**80%**				**2**
15		**70%**				**2**
16		**50%**				**2**
17		**25%**				**2**
18		**DRY (0%)**				**2**

3.2 Physical and Shear Strength Parameters

The shear strength parameters and physical properties of SS1 and SS2 sand are presented in Table 3.2. The internal friction angle was determined through direct shear tests on dry sand, with displacement rates set at 0.5 mm/min. The reported

values represent averages from three repeated tests conducted at varying normal stresses.

Table 3.2 Physical properties and Shear strength parameters for the sand.

Shear strength parameters	**c (kPa)**	**0**
	ϕ_{peak} dry, (degrees)	**34.06**
Physical properties	**Gs**	**2.68**
	Void ratio, e	**0.76**
	Coefficient of uniformity, cu	**4.46**
	Coefficient of curvature, cc	**1.27**
	e_{min}	**0.47**
	e_{max}	**0.83**

3.3 Direct Shear Results Under Normal Stress of SS1

3.3.1 (62.5) kPa Normal Stress

Figure 3.1 illustrates the shear strength against horizontal displacement of the mean of each degree of saturation tested for the 62.5kPa normal stress.

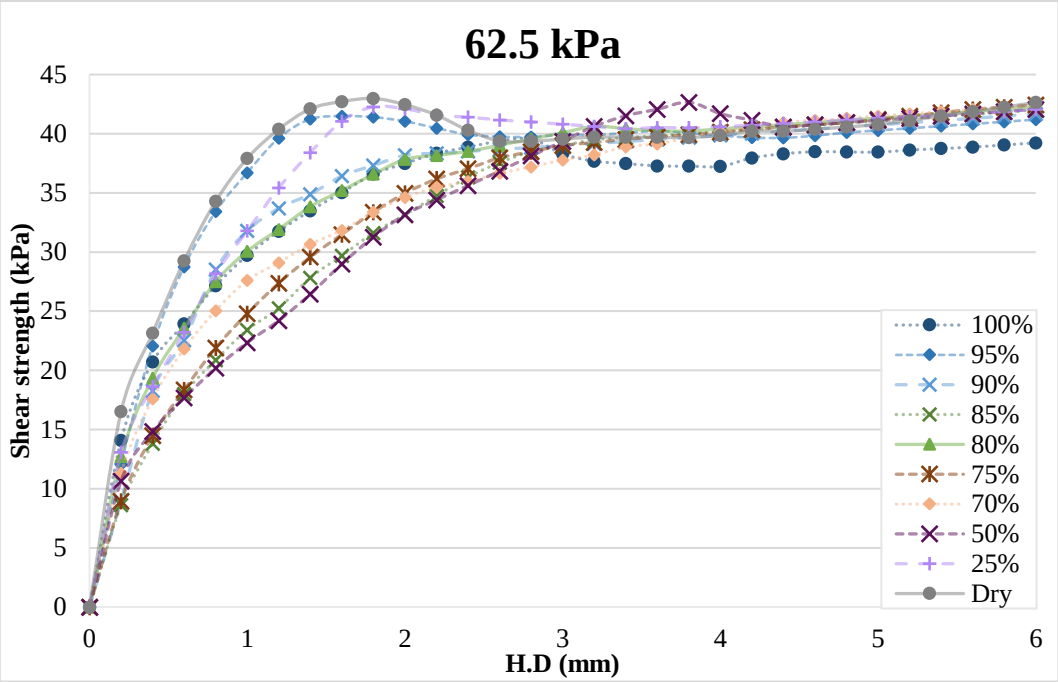

Figure 3.1 Shear strength against Horizontal displacement of SS1 under 62.5kPa normal stress.

3.3.2 (125) kPa Normal Stress

Figure 3.2 illustrates the shear strength against horizontal displacement of the mean of each degree of saturation tested for the 125kPa normal stress.

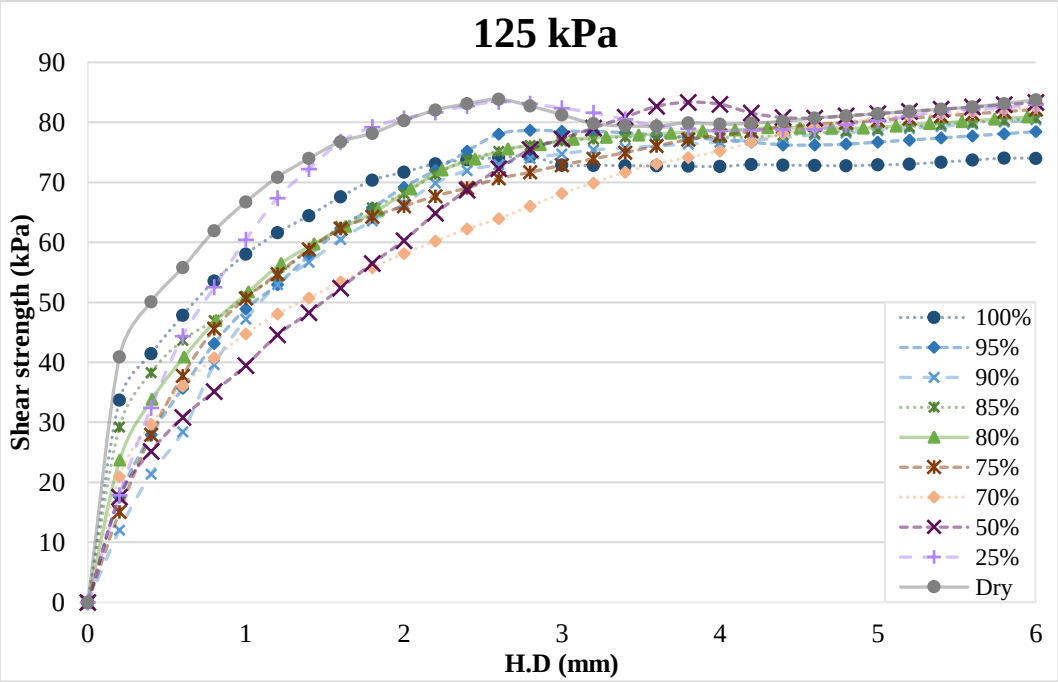

Figure 3.2 Shear strength against Horizontal displacement of SS1 under 125kPa normal stress.

3.3.3 (250) kPa Normal Stress

Figure 3.3 illustrates the shear strength against horizontal displacement of the mean of each degree of saturation tested for the 250kPa normal stress.

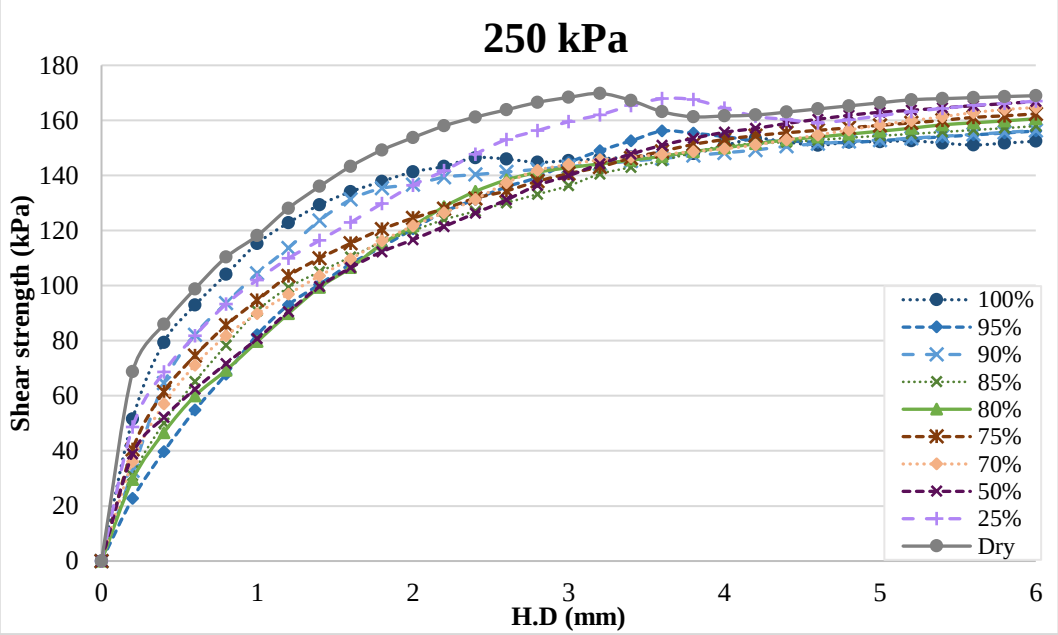

Figure 3.3 Shear strength against Horizontal displacement of SS1 under 250kPa normal stress.

3.4 Shear Strength Parameters of SS1

3.4.1 Fully Saturated (100% Degree of Saturation)

In Figure 3.4 the shear strength parameters are shown for peak and critical state (critical state is the state where the soil does not show an increase in shear, it usually starts showing that at 10% of the diameter of the sample) for fully saturated.

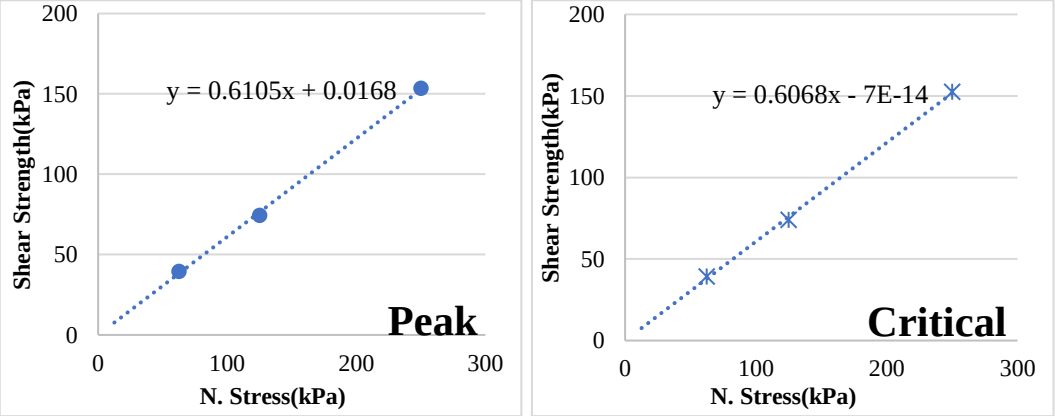

Figure 3.4 Failure envelope for 100% saturated condition of SS1.

	C (kPa)	Phi φ
Mean Peak	**0.00**	**31.17**
Mean Critical	**0.00**	**30.99**

Figure 3.4 Failure envelope for 100% saturated condition of SS1. (continued…).

3.4.2 Partially Saturated (95% Degree of Saturation)

In Figure 3.5 the shear strength parameters are shown for peak and critical states for 95% saturated case.

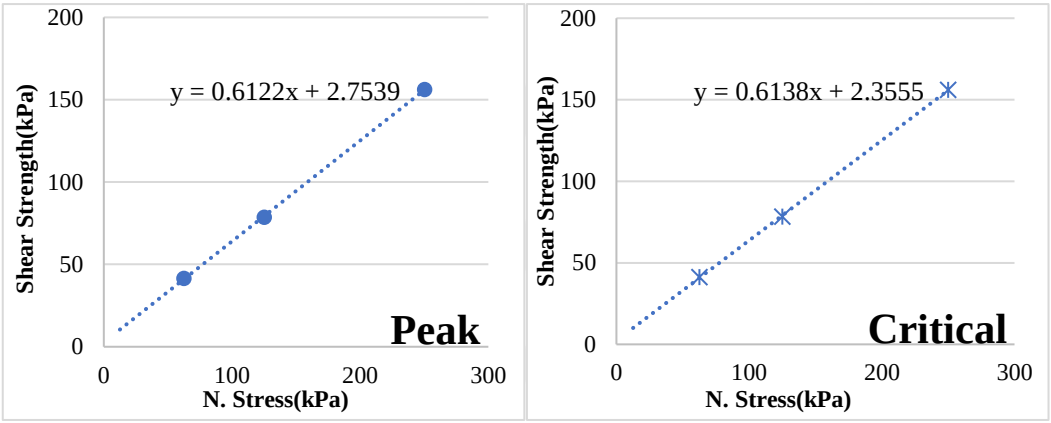

	C (kPa)	Phi φ
Mean Peak	**2.81**	**31.44**
Mean Critical	**2.39**	**31.51**

Figure 3.5 Failure envelope for 95% saturated condition of SS1.

3.4.3 Partially Saturated (90% Degree of Saturation)

Figure 3.6 shows shear strength parameters at peak and critical for 90% saturated case.

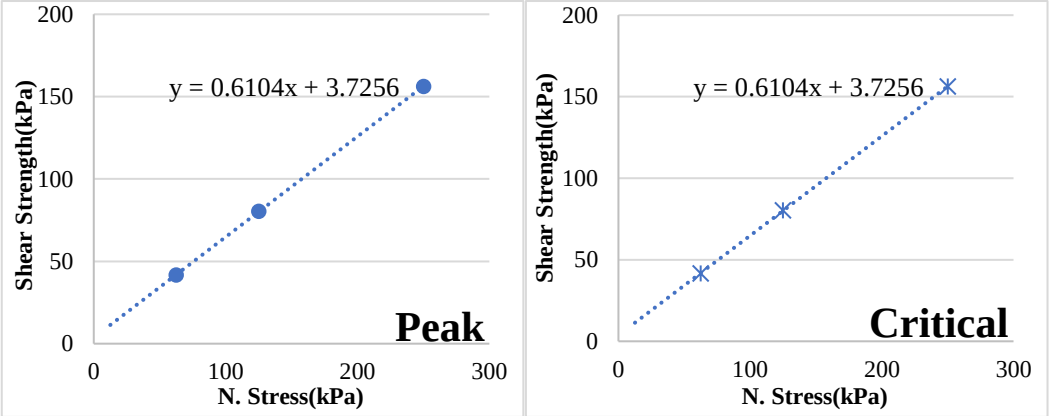

	c (kPa)	Phi φ
Mean Peak	**3.88**	**31.48**
Mean Critical	**3.88**	**31.48**

Figure 3.6 Failure envelope for 90% saturated condition of SS1.

3.4.4 Partially Saturated (85% Degree of Saturation)

Figure 3.7 shows the shear strength parameters at peak and critical for 85% saturation degree.

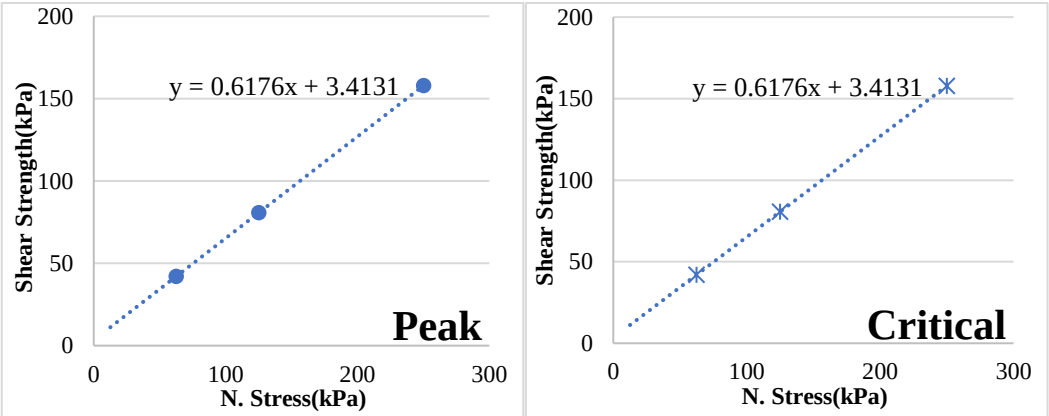

	c (kPa)	Phi φ
Mean Peak	**3.41**	**31.78**
Mean Critical	**3.41**	**31.78**

Figure 3.7 Failure envelope for 85% saturated condition of SS1.

3.4.5 Partially Saturated (80% Degree of Saturation)

Figure 3.8 shows the shear strength parameters at peak and critical for 80% saturated case.

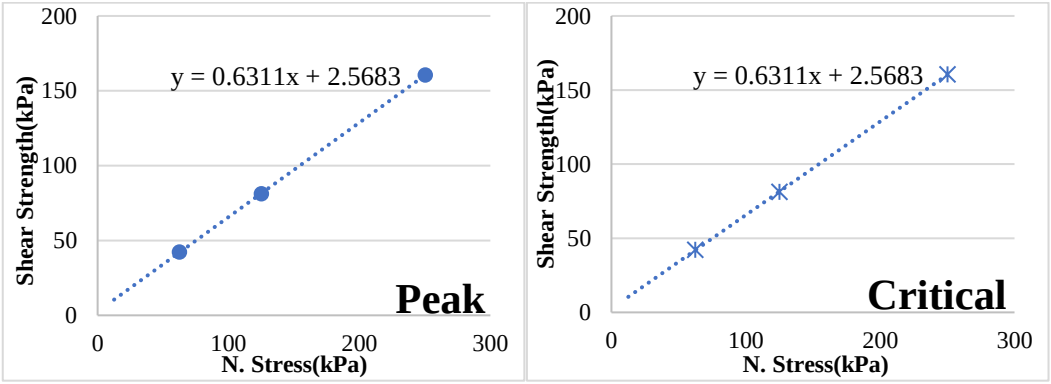

	c (kPa)	Phi φ
Mean Peak	**2.48**	**32.24**
Mean Critical	**2.48**	**32.24**

Figure 3.8 Failure envelope for 80% saturated condition of SS1.

3.4.6 Partially Saturated (75% Degree of Saturation)

Figure 3.9 shows the shear strength parameters for a 75% saturated case.

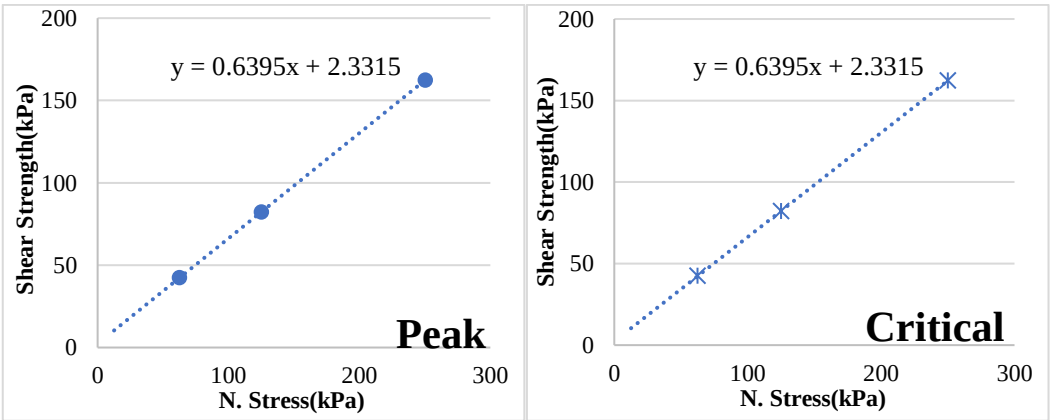

	c (kPa)	Phi φ
Mean Peak	**1.91**	**32.74**
Mean Critical	**1.91**	**32.74**

Figure 3.9 Failure envelope for 75% saturated condition of SS1.

3.4.7 Partially Saturated (70% Degree of Saturation)

Figure 3.10 shows the shear strength parameters for a 70% saturated case.

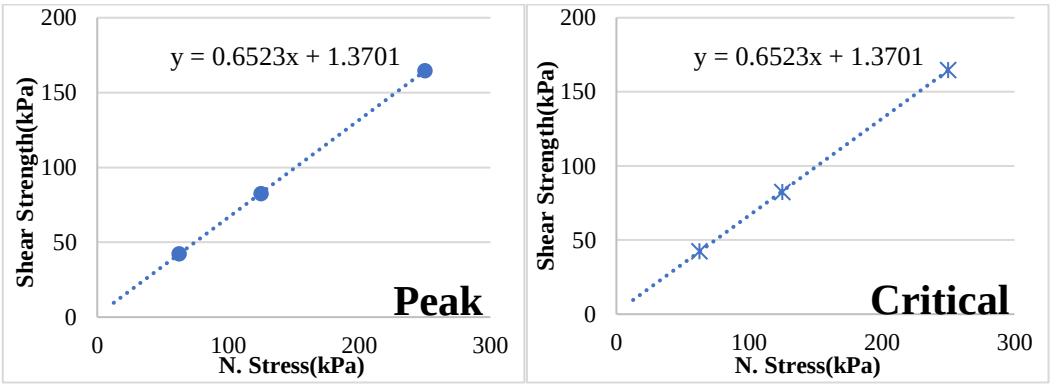

	c (kPa)	Phi φ
Mean Peak	**1.34**	**33.09**
Mean Critical	**1.34**	**33.09**

Figure 3.10 Failure envelope for 70% saturated condition of SS1.

3.4.8 Partially Saturated (50% Degree of Saturation)

Figure 3.11 shows the shear strength parameters for a 50% saturated case.

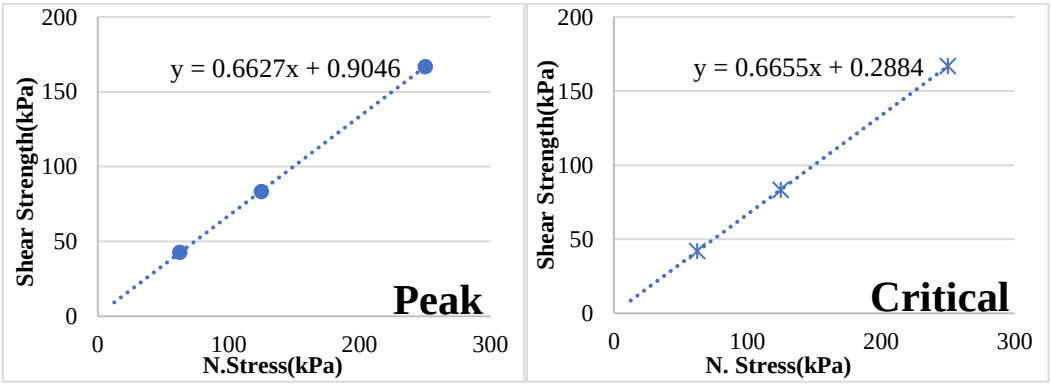

	c (kPa)	Phi φ
Mean Peak	**0.86**	**33.54**
Mean Critical	**0.39**	**33.63**

Figure 3.11 Failure envelope for 50% saturated condition of SS1.

3.4.9 Partially Saturated (25% Degree of Saturation)

Figure 3.12 shows the shear strength parameters at peak and critical for 25%S.

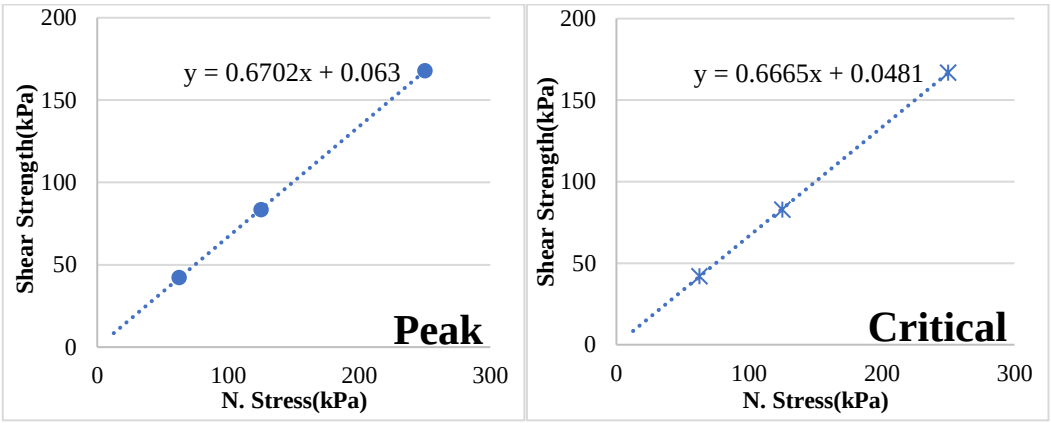

	c (kPa)	Phi φ
Mean Peak	**0.26**	**33.88**
Mean Critical	**0.02**	**33.80**

Figure 3.12 Failure envelope for 25% saturated condition of SS1.

3.4.10 Fully Dry (0% Degree of Saturation)

Figure 3.13 shows the shear strength parameters for a fully dry case.

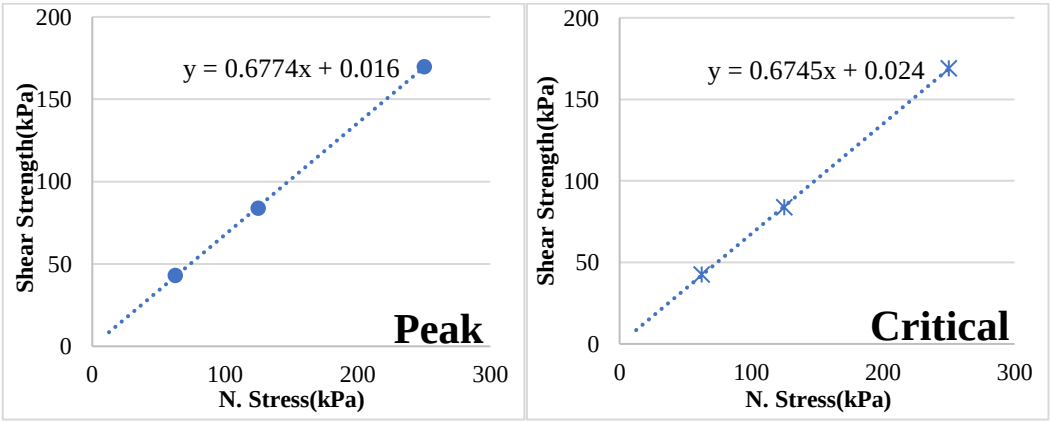

	c (kPa)	Phi φ
Mean Peak	**0.00**	**34.06**
Mean Critical	**0.00**	**33.84**

Figure 3.13 Failure envelope for Fully Dry condition of SS1.

3.5 Direct Shear Results Under Normal Stress of SS2

3.5.1 (62.5) kPa Normal Stress

Figure 3.14 illustrates the shear strength against horizontal displacement for all degrees of saturation tested for SS2 under 62.5kPa normal stress.

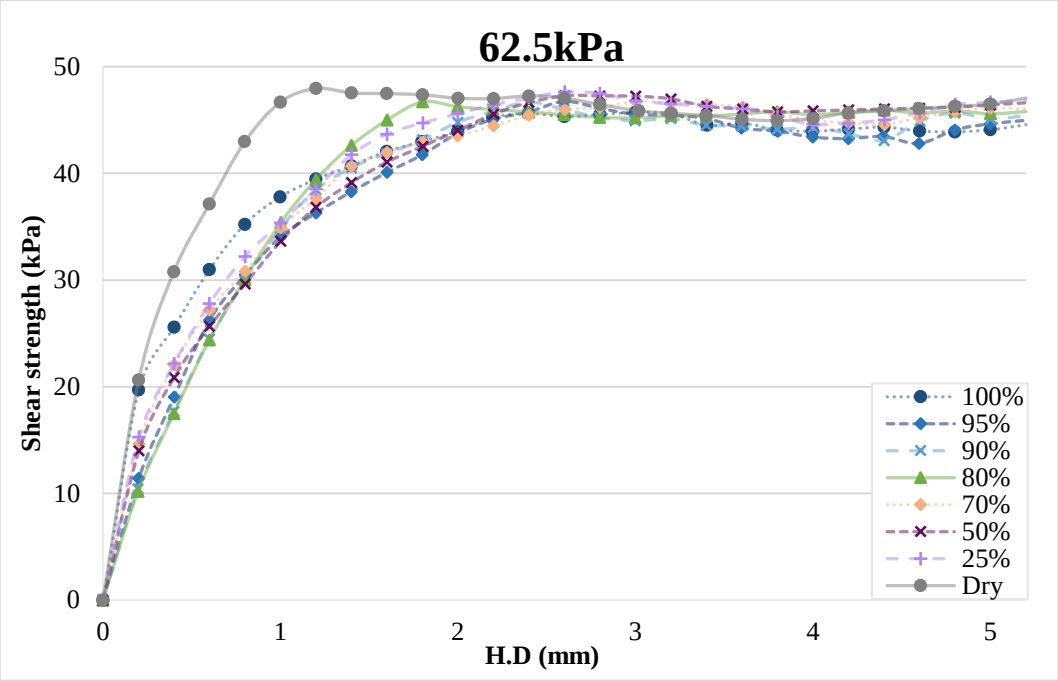

Figure 3.14 Shear strength against Horizontal displacement of SS2 under 62.5kPa normal stress.

3.5.2 (125) kPa Normal Stress

Figure 3.15 illustrates the shear strength against horizontal displacement for all degrees of saturation tested for SS2 under 125kPa normal stress.

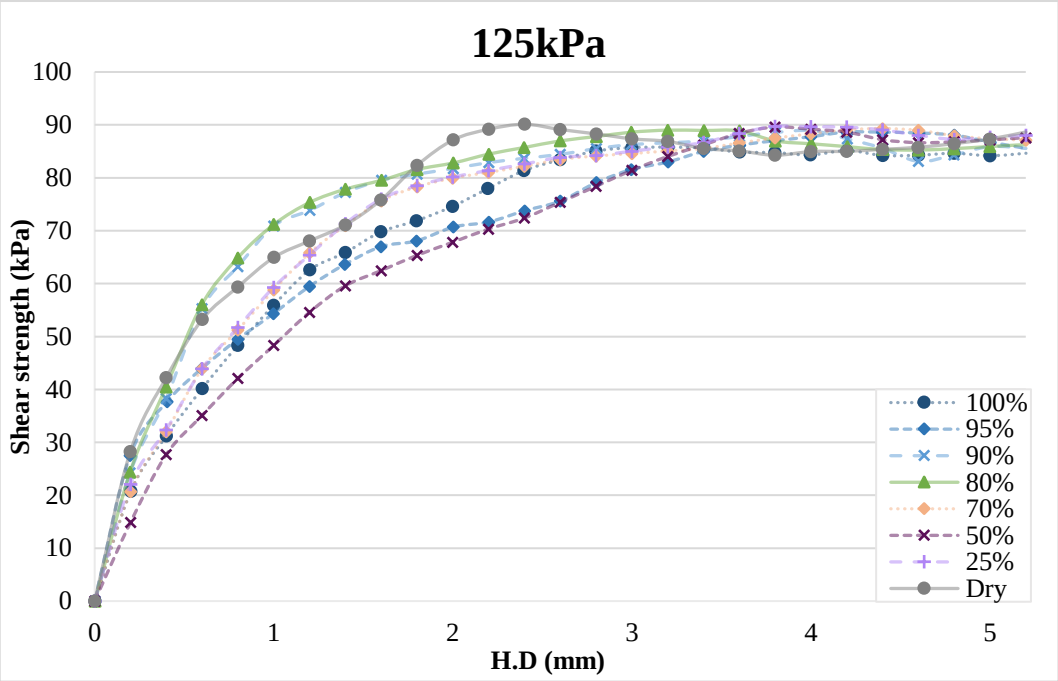

Figure 3.15 Shear strength against Horizontal displacement of SS2 under 125kPa normal stress.

3.5.3 (250) kPa Normal Stress

Figure 3.16 illustrates the shear strength against horizontal displacement for all degrees of saturation tested for SS2 under 250kPa normal stress.

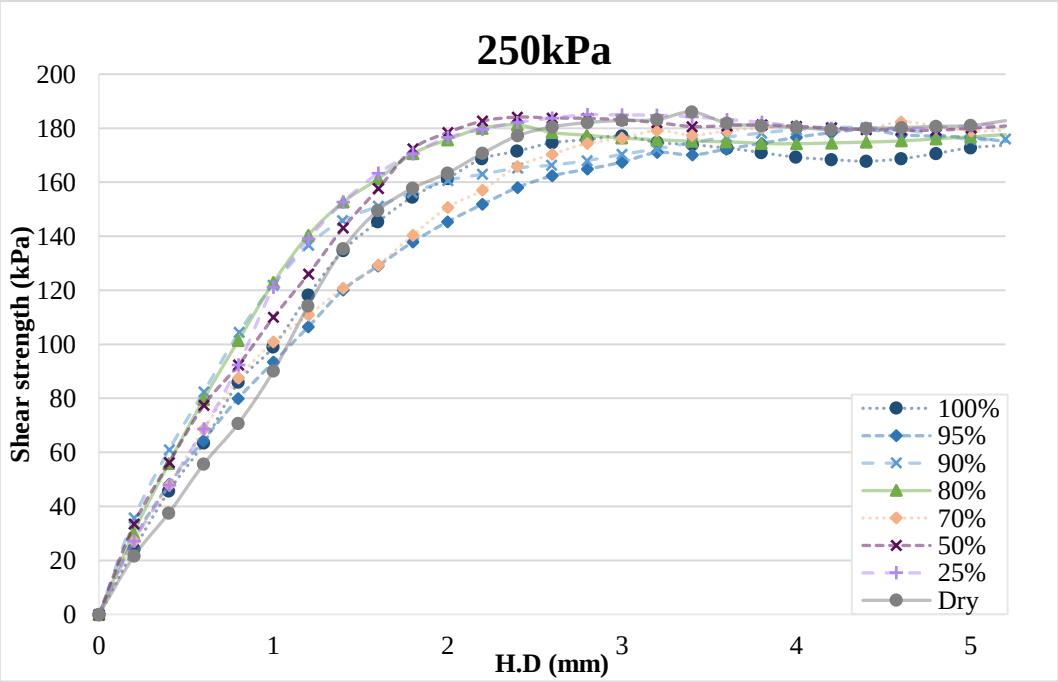

Figure 3.16 Shear strength against Horizontal displacement of SS2 under 250kPa normal stress.

3.6 Shear Strength Parameters of SS2

3.6.1 Fully Saturated (100% Degree of Saturation)

Figure 3.17 shows the shear strength parameters at peak and critical for SS2 with a relative density of 65%.

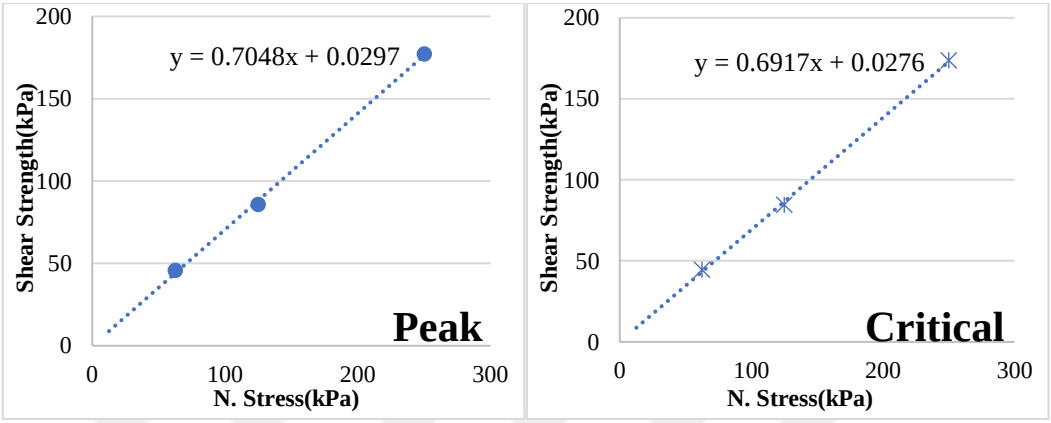

	c (kPa)	Phi φ
Mean Peak	**0**	**35.18**
Mean Critical	**0**	**34.67**

Figure 3.17 Failure envelope for the Fully saturated condition of SS2.

3.6.2 Partially Saturated (95% Degree of Saturation)

Figure 3.18 shows the shear strength parameters at peak and critical for SS2 with relative density of 65%.

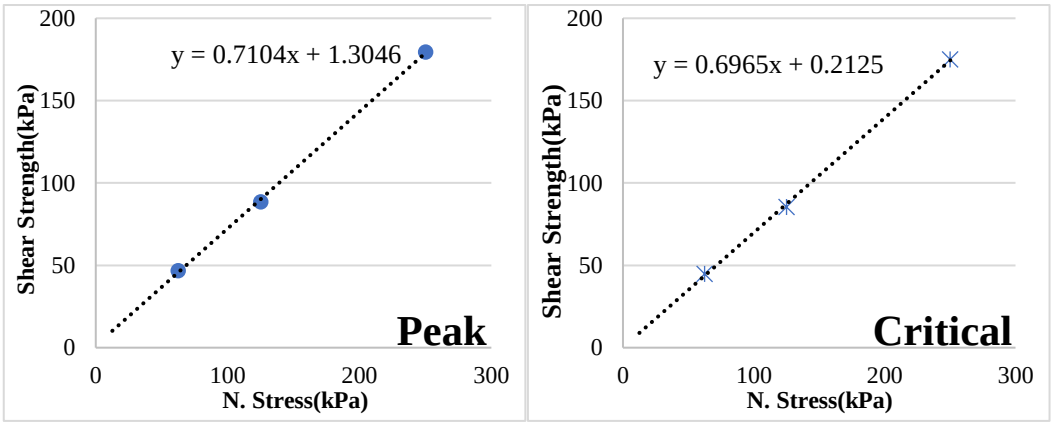

	c (kPa)	Phi φ
Mean Peak	**1.30**	**35.39**
Mean Critical	**0.21**	**34.86**

Figure 3.18 Failure envelope for 95% saturated condition of SS2.

3.6.3 Partially Saturated (90% Degree of Saturation)

Figure 3.19 shows the shear strength parameters at peak and critical for SS2.

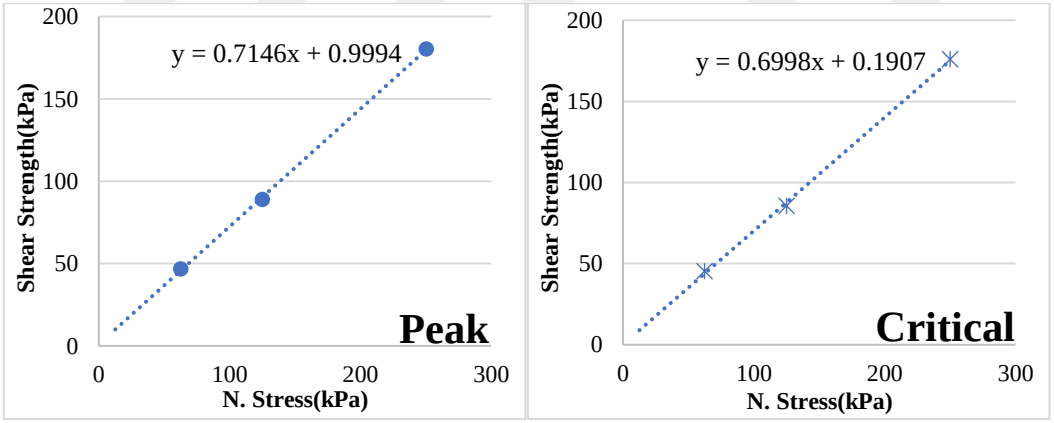

	c (kPa)	Phi φ
Mean Peak	**1.00**	**35.55**
Mean Critical	**0.19**	**34.99**

Figure 3.19 Failure envelope for 90% saturated condition of SS2.

3.6.4 Partially Saturated (80% Degree of Saturation)

Figure 3.20 the peak and critical shear strength parameters are shown for SS2.

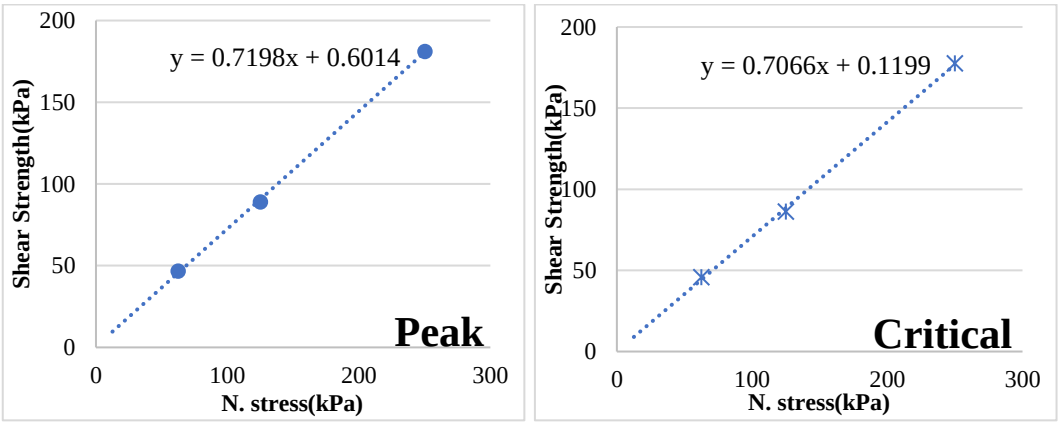

	c (kPa)	Phi φ
Mean Peak	**0.60**	**35.75**
Mean Critical	**0.12**	**35.24**

Figure 3.20 Failure envelope for 80% saturated condition of SS2.

3.6.5 Partially Saturated (70% Degree of Saturation)

Figure 3.21 the peak and critical shear strength parameters are shown for SS2.

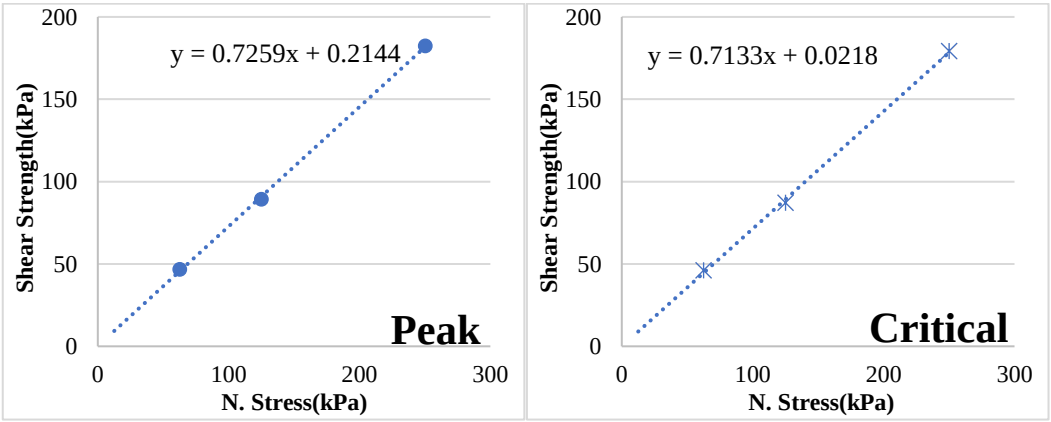

	c (kPa)	Phi φ
Mean Peak	**0.21**	**35.98**
Mean Critical	**0.02**	**35.50**

Figure 3.21 Failure envelope for 70% saturated condition of SS2.

3.6.6 Partially Saturated (50% Degree of Saturation)

Figure 3.22 The peak and critical shear strength parameters are shown for SS2 with a relative density of 65%.

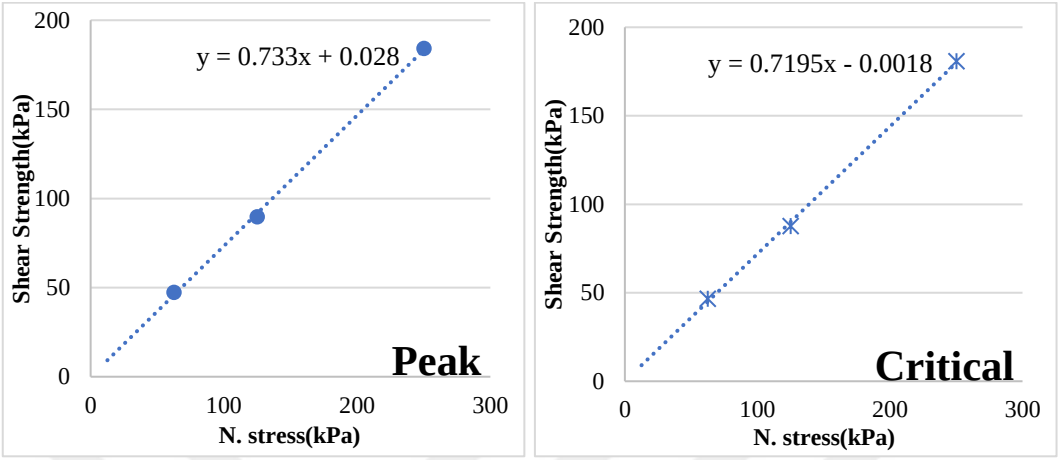

	c (kPa)	Phi φ
Mean Peak	**0.03**	**36.24**
Mean Critical	**0**	**35.74**

Figure 3.22 Failure envelope for 50% saturated condition of SS2.

3.6.7 Partially Saturated (25% Degree of Saturation)

Figure 3.23 The peak and critical shear strength parameters are shown for SS2 with a relative density of 65%.

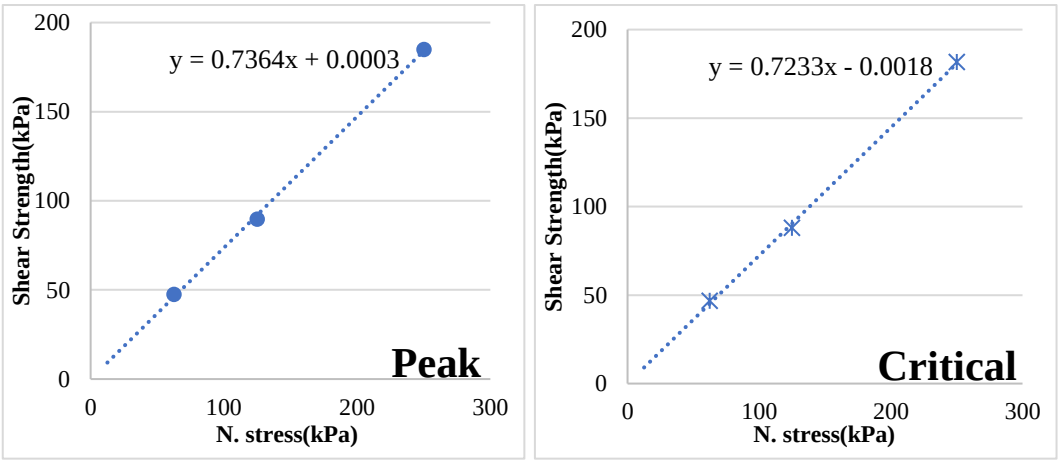

	c (kPa)	Phi φ
Mean Peak	**0**	**36.37**
Mean Critical	**0**	**35.88**

Figure 3.23 Failure envelope for 25% saturated condition of SS2.

3.6.8 Fully Dry (0% Degree of Saturation)

Figure 3.24 The peak and critical shear strength parameters are shown for SS2 with a relative density of 65%.

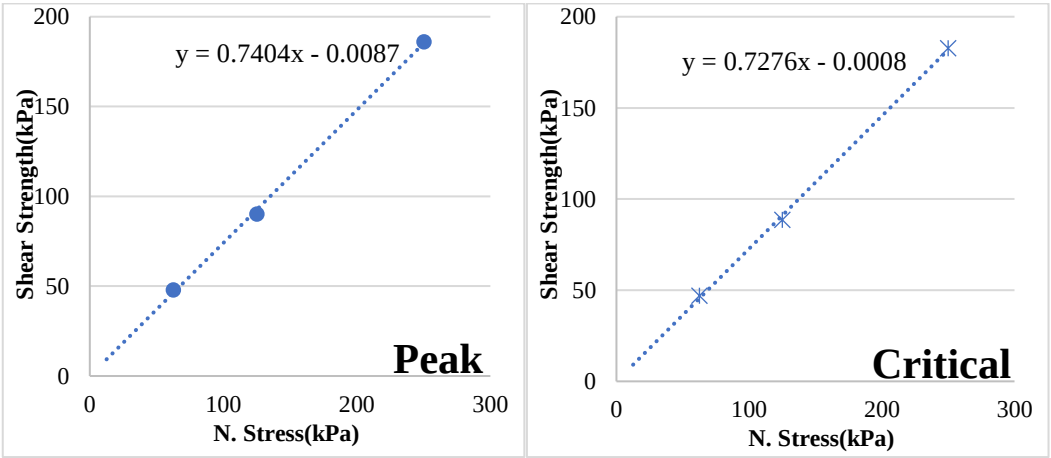

	c (kPa)	Phi φ
Mean Peak	**0**	**36.52**
Mean Critical	**0**	**36.04**

Figure 3.24 Failure envelope for Fully Dry condition of SS2.

3.7 Data Comparison

3.7.1 Shear Strength Parameters of SS1

The peak and critical cohesion and angle of friction of all the saturation (100%, %95, 90%, 85%, 80%, 75%, 70%, 50%, 25%, and dry) cases of the SS1 sand sample with a relative density of (35%) is shown in the Table 3.3 below, the relation of these different parameters is illustrated in the graph in Figures 3.25 and 3.26.

Table 3.3 Comparison of all the shear strength parameters for SS1.

Saturation degree	Mean Peak		Mean Critical	
	c	Phi	c	Phi
100%	0.00	31.17	0.00	30.99
95%	2.81	31.44	2.39	31.51
90%	3.88	31.48	3.88	31.48
85%	3.41	31.78	3.41	31.78
80%	2.48	32.24	2.48	32.24
75%	1.91	32.74	1.91	32.74
70%	1.34	33.09	1.34	33.09
50%	0.86	33.54	0.39	33.63
25%	0.26	33.88	0.02	33.80
0%	0.00	34.06	0.00	33.84

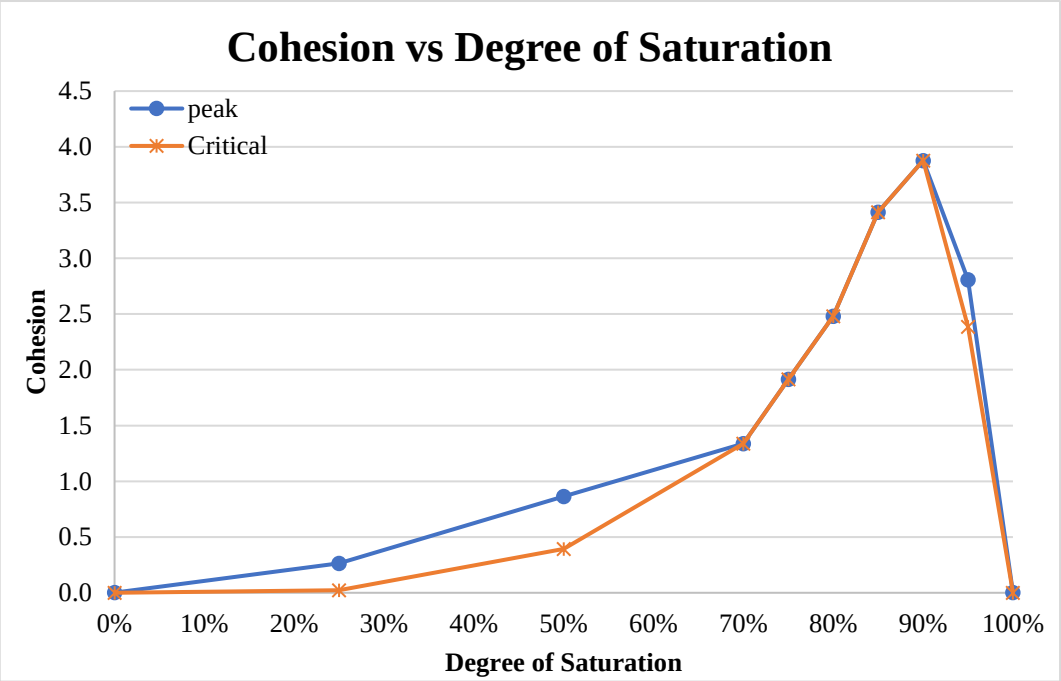

Figure 3.25 Cohesion vs all the degrees of saturation for SS1.

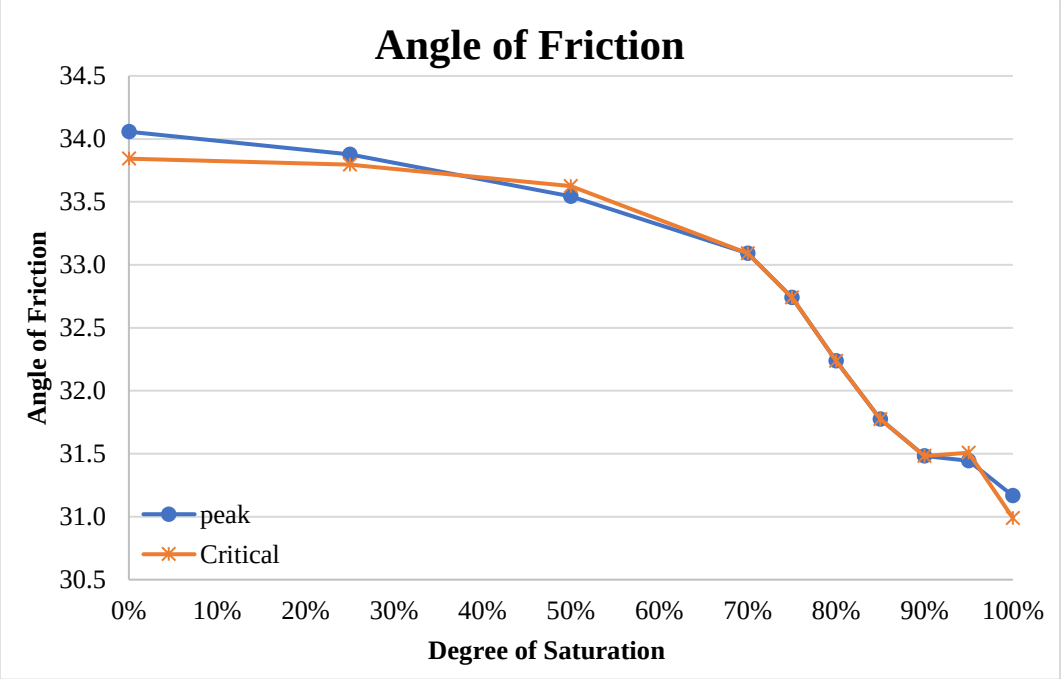

Figure 3.26 Angle of friction vs all the degrees of saturation of SS1

3.7.2 Shear Strength Values of SS1

The values of peak and critical shear strength for the degree of saturation (100%, %95, 90%, 85%, 80%, 75%, 70%, 50%, 25%, and dry) of the SS1 sand sample with a relative density of (35%) are shown in Table 3.4, the saturation degree effect on shear strength is illustrated in the Figures 3.27 and 3.28.

Table 3.4 Shear strength values of all the degrees of saturation for SS1.

Saturation degree	Mean Peak			Mean Critical		
	62	125	250	62	125	250
100%	39.26	73.52	152.03	39.07	72.88	151.01
95%	41.49	78.64	156.01	41.13	78.45	155.95
90%	42.00	80.75	156.99	42.00	80.75	156.99
85%	42.13	80.94	158.37	42.13	80.94	158.37
80%	42.16	81.01	160.37	42.16	81.01	160.37
75%	42.26	82.16	162.84	42.26	82.16	162.84
70%	42.22	82.67	164.44	42.22	82.67	164.44
50%	42.60	83.39	166.86	42.16	83.33	166.86
25%	42.55	83.81	168.38	42.13	83.39	167.60
0%	42.57	84.14	169.26	42.06	83.73	167.82

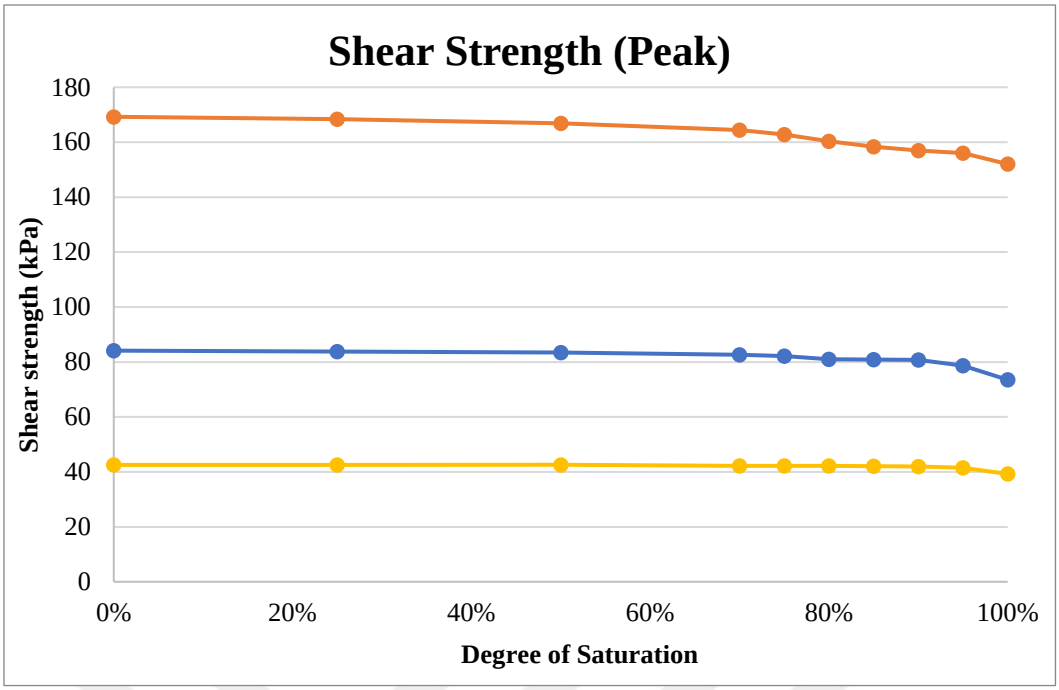

Figure 3.27 Peak shear strength values for SS1 under different degrees of saturation.

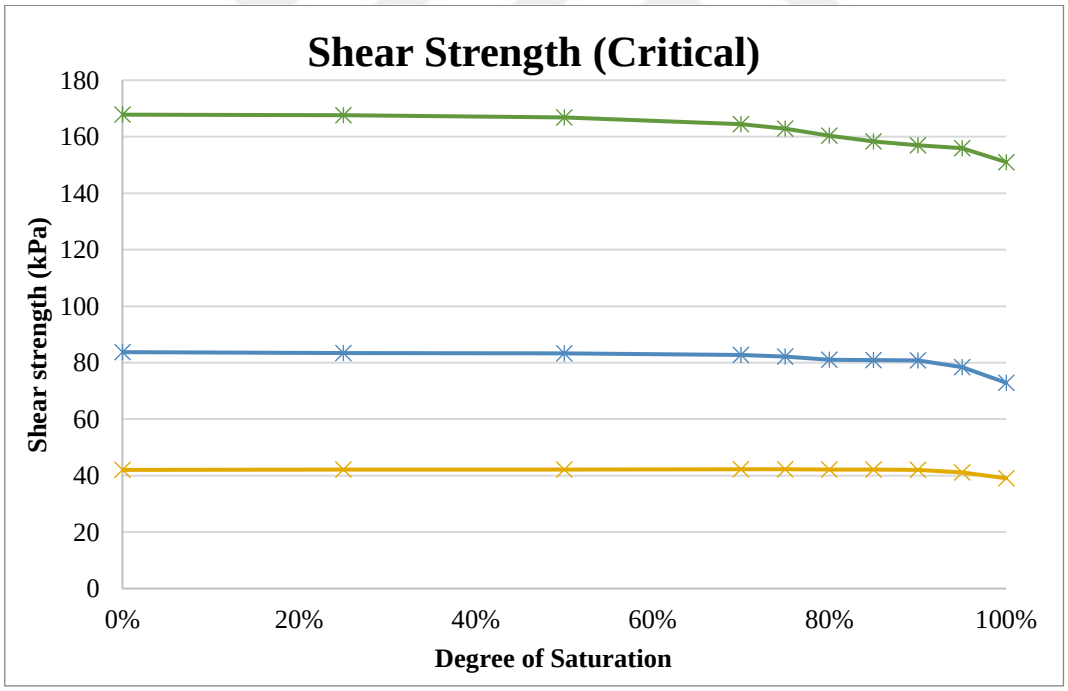

Figure 3.28 Critical shear strength values for SS1 under different degrees of saturation.

3.7.3 Shear Strength Parameters of SS2

The peak and critical cohesion and angle of friction of all the saturation levels 100, 95%, 90%, 80%, 70%, 50%, 25%, and dry cases of the SS2 sand sample with a

relative density of (65%) is shown in Table 3.5 below, the relation of these different parameters is illustrated in the graph in Figure 3.29 and 3.30.

Table 3.5 Comparison of all the shear strength parameters for SS2.

Saturation degree	Mean Peak		Mean Critical	
	c	Phi	c	Phi
100%	0	35.18	0	34.67
95%	1.30	35.39	0.21	34.86
90%	1.00	35.55	0.19	34.99
80%	0.60	35.75	0.12	35.24
70%	0.21	35.98	0.02	35.50
50%	0.03	36.24	0.00	35.74
25%	0.00	36.37	0.00	35.88
0%	0	36.52	0	36.04

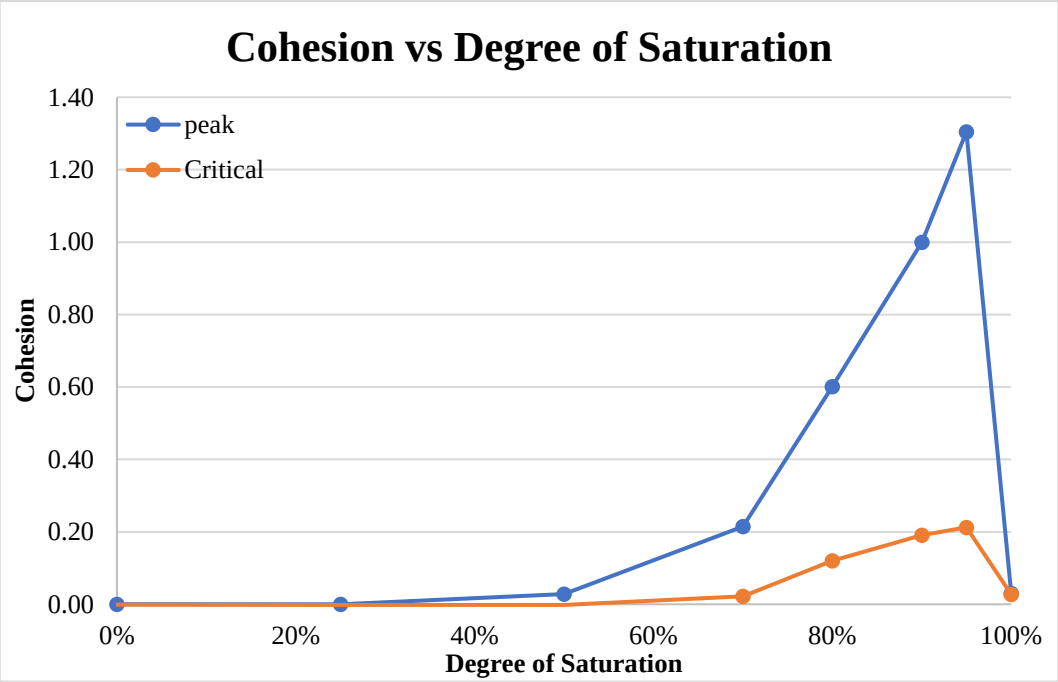

Figure 3.29 Cohesion vs all the degrees of saturation for SS2.

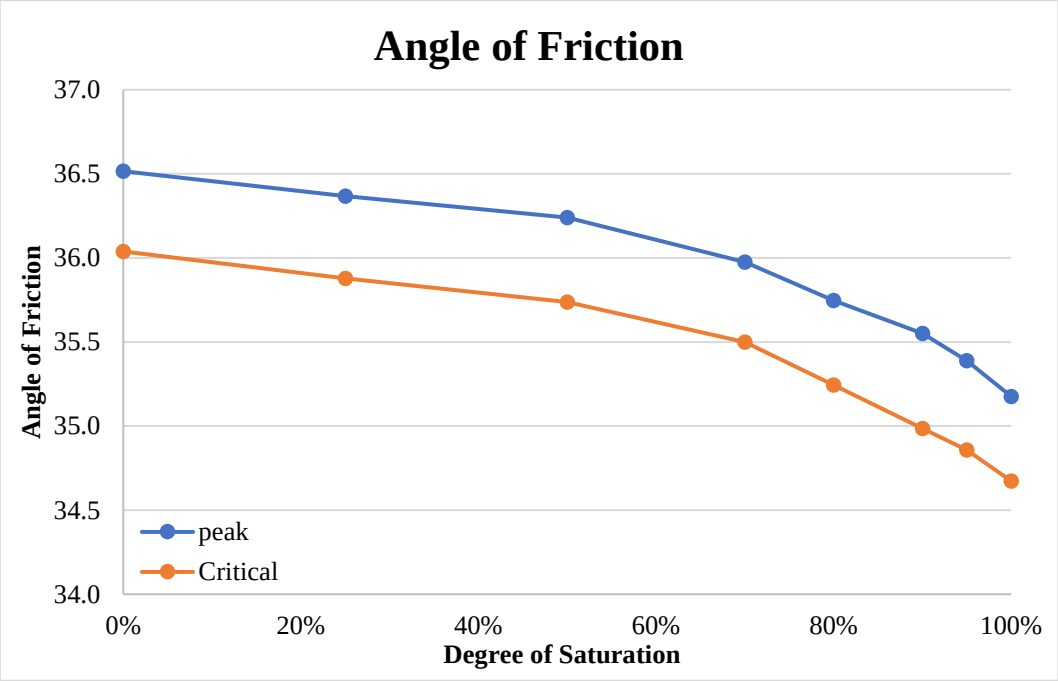

Figure 3.30 Angle of friction vs all the degrees of saturation of SS2.

3.7.4 Shear Strength Values of SS2

The peak and critical shear strength values of the degree of saturation (100%, %95, 90%, 80%, 70%, 50%, 25%, and dry) of the SS2 sand sample with a relative density of (65%) are shown in Table 3.6, the saturation degree effect on shear strength is

illustrated in the Figures 3.31 and 3.32.

Table 3.6 Shear strength values of all the degrees of saturation for SS2.

Saturation degree	Mean Peak			Mean Critical		
	62	125	250	62	125	250
100%	45.71	85.80	177.15	44.57	84.64	173.72
95%	46.74	88.65	179.53	44.97	85.55	175.06
90%	46.68	88.91	180.28	45.42	85.55	176.00
80%	46.71	89.01	181.23	45.79	86.28	177.63
70%	46.74	89.32	182.38	46.03	87.15	179.17
50%	47.28	89.60	184.11	46.62	87.57	180.82
25%	47.64	89.74	185.01	46.86	88.05	181.76
0%	47.95	90.12	186.04	47.07	88.66	182.80

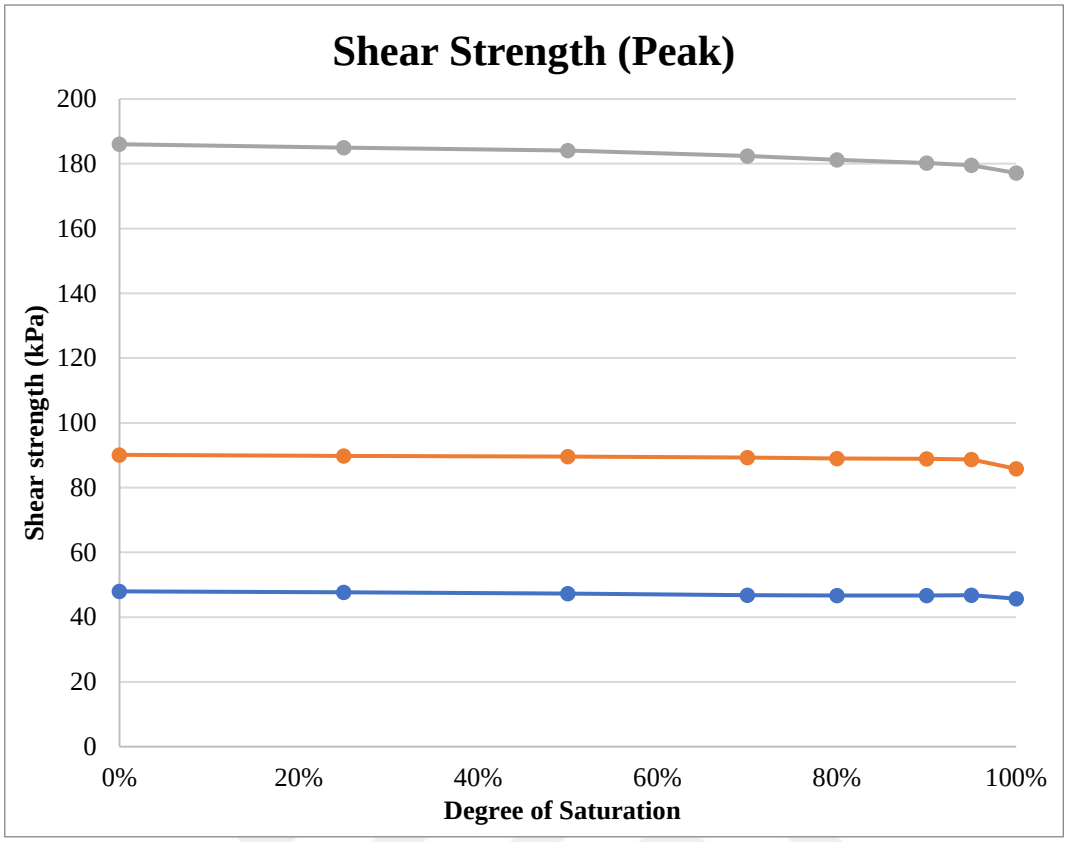

Figure 3.31 Peak shear strength values for SS2 under different degrees of saturation.

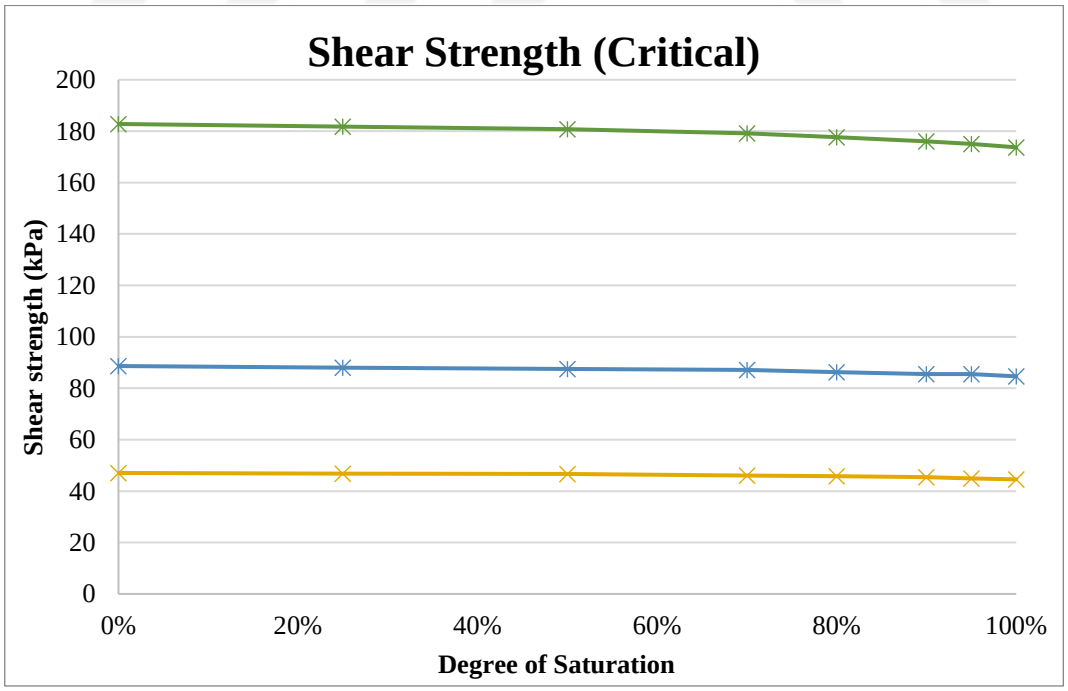

Figure 3.32 Critical shear strength values for SS2 under different degrees of saturation.

3.8 Vertical Displacement Graphs

3.8.1 Volume Change of SS1

The vertical change which is also known as dilation is shown in Figures 3.33, 3.34, and 3.35 for SS1 under (62.5, 125, 250)kPa normal stress respectively.

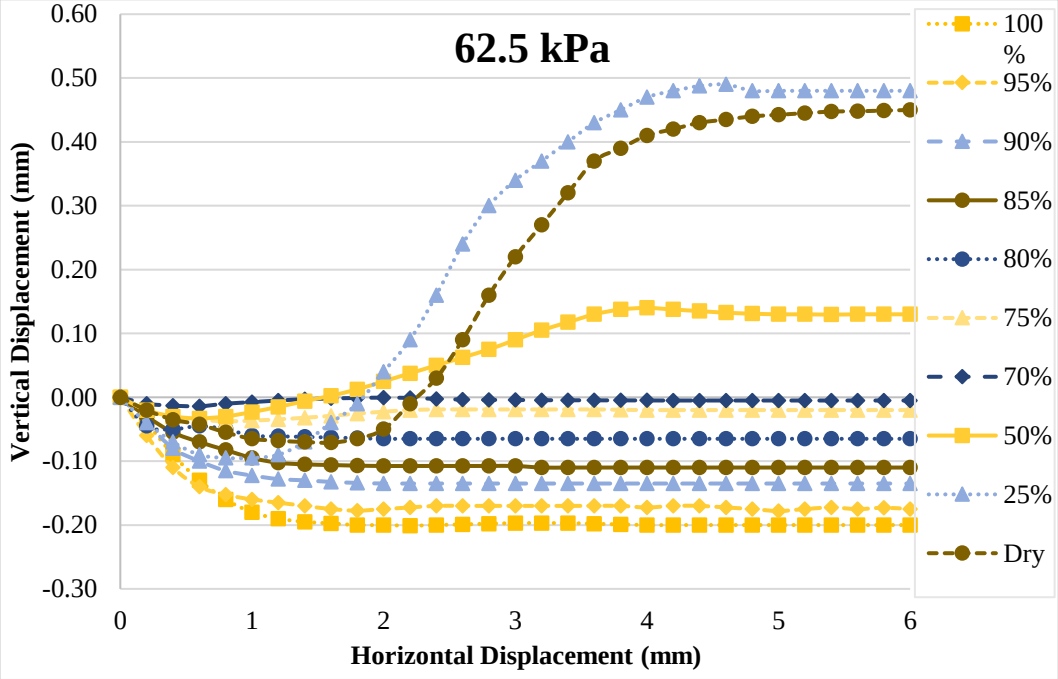

Figure 3.33 Horizontal vs Vertical displacement of all the degrees of saturation for SS1 under 62.5kPa normal stress.

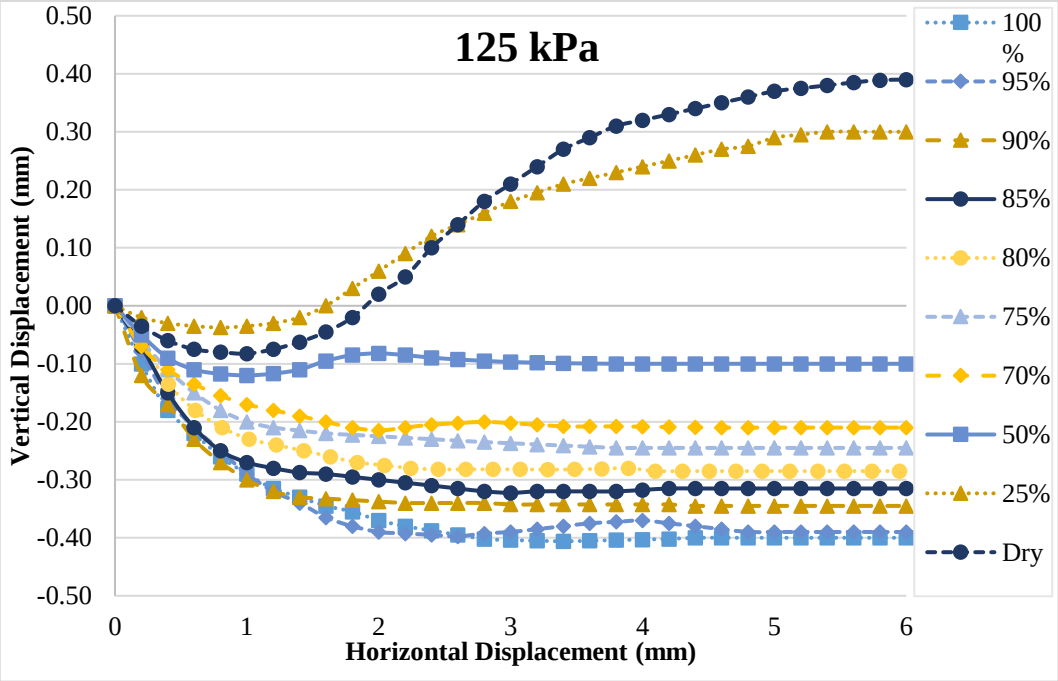

Figure 3.34 Horizontal vs Vertical displacement of all the degrees of saturation for SS1 under 125kPa normal stress.

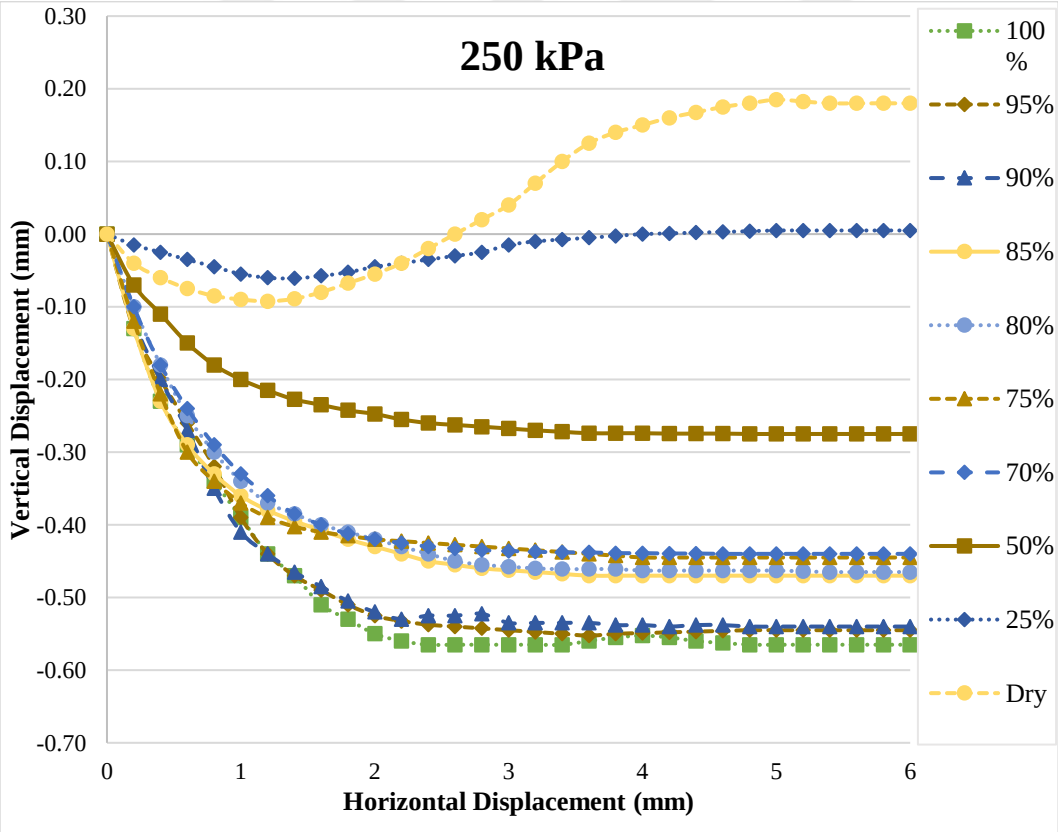

Figure 3.35 Horizontal vs Vertical displacement of all the degrees of saturation for SS1 under 250kPa normal stress.

3.9 Image Analysis

The sand particle size of (2-0.85)mm showed an average roundness of (0.72) after the ImageJ analysis, an image of the particle shape is shown in Figure 3.36. The sand particle size of (4.75-2)mm showed an average roundness of (0.73) after the ImageJ analysis, an image of the particle shape shown in Figure 3.37, this value typically indicates that the particles are not highly angular but are also not completely rounded. Sands with such a roundness tend to have a slightly reduced interlocking capability compared to angular sands, leading to a lower angle of internal friction which explains that the sand particle we have is semi-rounded, the semi-rounded sand is assumed to have the angle of friction between 29 to 35, These values are general estimates. For precise determination, lab testing such as a direct shear test or triaxial test would be required, because there are other factors like grain size distribution, compaction, and moisture content that have to be taken into account.

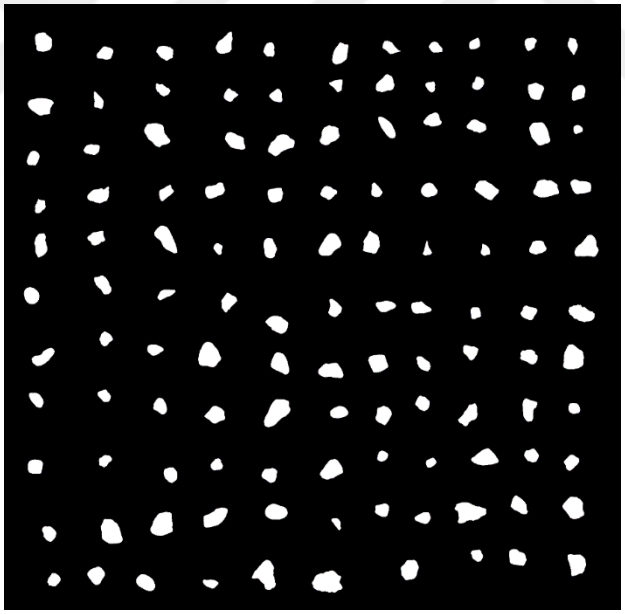

Figure 3.36 Particle's size of (2-0.85)mm under ImageJ.

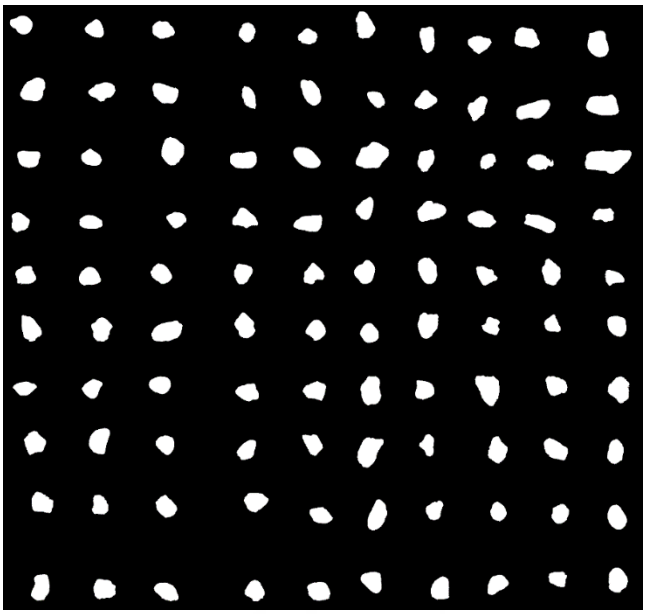

Figure 3.37 Particle's size of (4.75-2)mm under ImageJ.

4
CONCLUSION

The behavior of fine grain soil or sand at a high degree of saturation is and has been of major interest in Geotechnical engineering because of soil's sensitivity in that condition. Due to the lowering of the water content in voids between Sand particles under the effect of temperature, Suction occurs that affects the behavior of sand to show more strength compared to fully saturated conditions for the same material. Plus, the surface tension of the surface of the water also plays a role in the strong behavior meanwhile, the dry case shows a high shear strength and angle of friction which shows that the fully saturated case is more critical.

The internal friction angle values and cohesion increase and decrease with the change in saturation rate and the value of the normal stresses. The peak was observed at different times, and the delay of the peak is due to the time it takes for the stability of particles while climbing upon each other. The compression and rearranging of particles at the beginning of the shearing is followed by dilation where the particles climb the next particle or aggregated chunk of particles that leads to a delayed peak. There is a stick-slip occurrence observed from the graph that shows a sudden temporary small loss of strength due to the slipping of sand particles upon each other in drier samples.

Comparison between the peak and critical shear strength parameters of all the saturation level cases of the SS1 with (35%)Dr and SS2 with (65%)Dr sand samples is illustrated in the graphs in Figures 4.1 and 4.2

An increase in the saturation rate leads to a decrease in the angle of friction with around 3° for SS1 loose sand with a relative density of 35% and 1.5° for SS2 the medium dense case with a relative density of 65%, that is due to fiction drier cases tend to have more friction between the particles meanwhile as the degree of saturation gets closer to fully saturated particles tend to slip and rearrange. Fully

saturated soil particles would have more freedom and movement unlike in unsaturated when suction has tied the particles together.

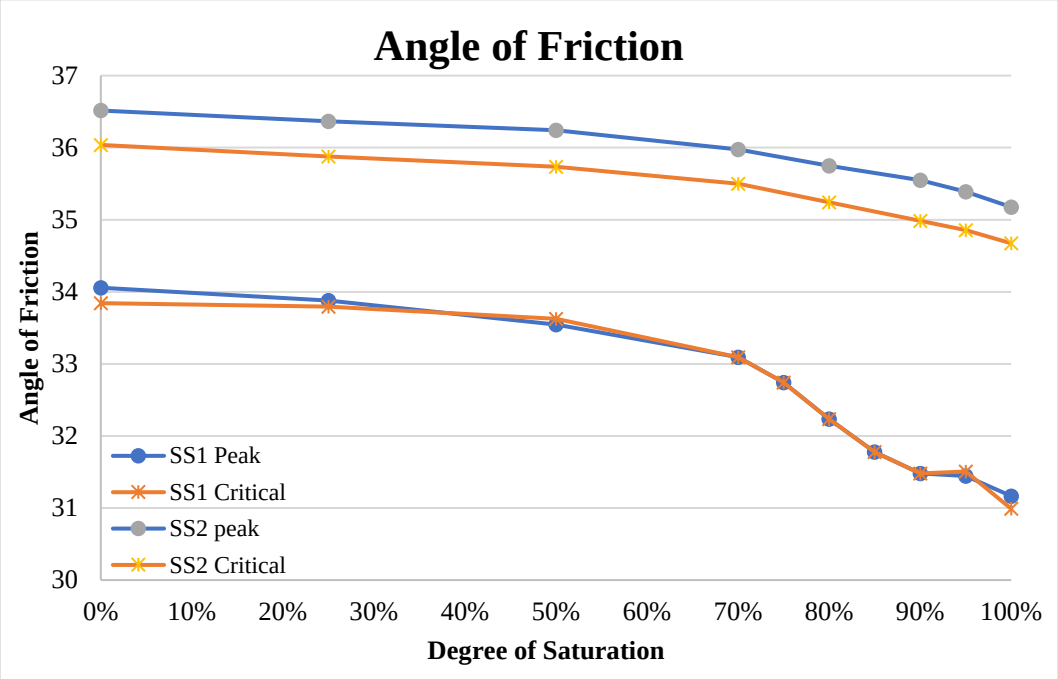

Figure 4.1 Comparison between SS1 and SS2 in Angle of friction vs all the degrees of saturation graph.

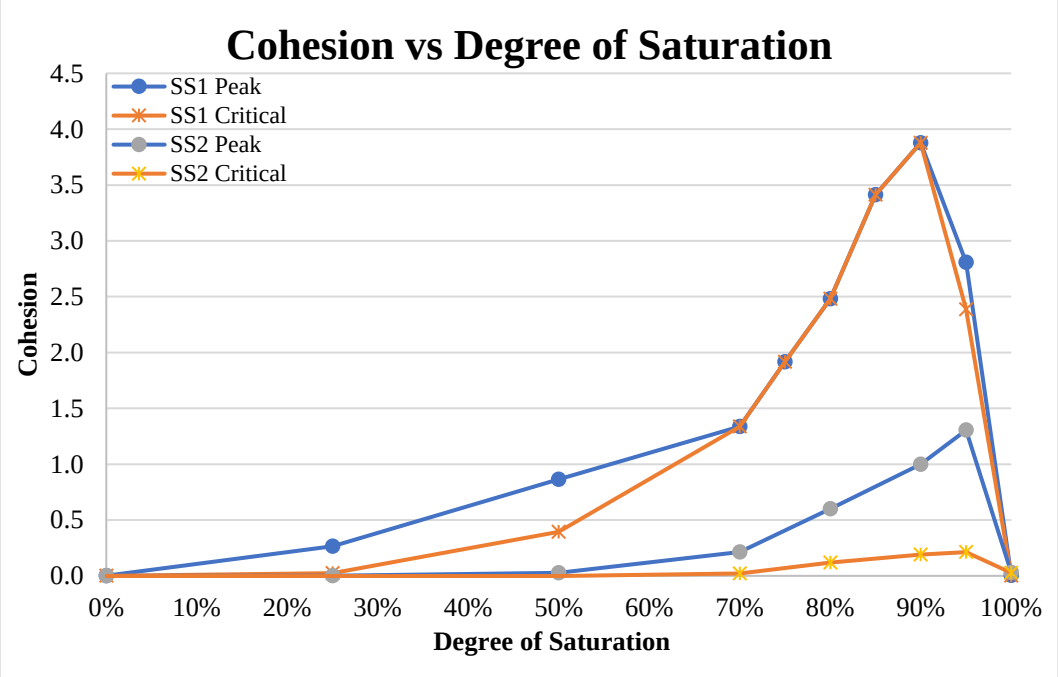

Figure 4.2 Comparison between SS1 and SS2 in Cohesion vs all the degree of saturation graph.

Cohesion showed slightly which was assumed to be suction as a particle is mostly sand, the possibility of cohesion was not available, but suction was behaving like

cohesion and showed in the graph in the zone between fully saturated and 70% saturation which is considered to be the suction affected zone.

Peak cohesion which as discussed considers suction showed a 90% saturation for the soil at a Dr of 35%, but as the sample was compacted to reach the Dr of 65% the peak was observed to be at 95% degree of saturation, which means the suction effect was lessening to all the degree of saturation and the peak moved closer to fully saturated because the volume for that trapped air within the particle was listening along with the water content.

Through the test, there was a focus on observing wetting collapse which is a case where particles aggregate and form bigger particles and break causing sudden collapse, but it showed only once true all the tests made that's why it was not taken into account, assuming that the type of soil was not required one.

Dilation in saturated case was not showing while dilation was observed in dry cases and 25%S as the soil was drier more dilation was showing, meanwhile 100% until 70% showed no dilation, and the greater the saturation degree the more volume change was observed which means the soil was consolidating due to slipping and rearrangement this case know as slip of particles and the dryer the sample the more dilation was showing which means particle were climbing on top of each other. Bigger dilation doesn’t necessarily mean bigger shear strength. It is probably due to aggregation collapse.

*There is the phenomenon of aggregation of sand particles due to the effect of van der Waals forces that creates a chunk of sand stick together behaving as on big particle that dilates and shows an early drop in the shear strength and gives in return lower internal angular friction. There are cases of the collapse of the aggregated particles due to a high amount of normal stress that results in the sudden loss of strength behavior. Observations have been made on one point that deserves to be in focus, and that is the accident of wetting collapse which seems to be more probable to occur in highly saturated sand. When there are big voids filled with water particles suddenly tend to fall into those gaps under the effect of external forces that trigger the movement especially when sheared. This may result in collapses that have been reported on roads, under the superstructures, and so on. Unfortunately wetting collapse was not observed at high unsaturated samples when small normal stress is applied.

Future research will employ distinct techniques and experiments that will not be possible to complete in the allotted time (actual data experiments typically take three days to complete). Further research could delve deeper into the mechanisms and experiment with various soil gradings to watch the wetness collapse and determine which range of particles primarily influences the behavioral shift. A mixture of soil will not give so accurate results, but the mostly different range of particle size and observing it with image analysis can help understand cases like wetting collapse, sudden failure, or the slip of particles while shearing.

REFERENCE

[1] M. A. Carter, Soil Sampling and Methods of Analysis. Pinawa, Manitoba: Canadian Society of Soil Science, 2008, p. 939.

[2] K. Terzaghi, R. B. Peck, and G. Mesri, Soil Mechanics in Engineering Practice. New York, NY, USA: John Wiley & Sons, Inc, 1996.

[3] T. W. Lambe and R. V. Whitman, Soil Mechanics. New York, NY, USA: John Wiley & Sons, Inc, 1991.

[4] N. Lu and W. J. Likos, Unsaturated Soil Mechanics. Hoboken, NJ, USA: Wiley, 2004.

[5] W. Ahmad and T. Uchimura, "The effect of moisture content at compaction and grain size distribution on the shear strength of unsaturated soils," Sustainability, vol. 15, no. 8, p. 5123, 2023.

[6] D. Sarker, M. Goudarzy, and D. König, "An interpretation of the influence of particle shape on the mechanical behavior of granular material," Granular Matter, vol. 21, no. 3, p. 245, 2019.

[7] Y. Mahmmoudi, A. C. Taiba, L. Hazout, and M. Belkhatir, "Packing density and overconsolidation ratio effects on the mechanical response of granular soils," Acta Geotechnica, vol. 14, no. 6, pp. 1427-1440, 2019.

[8] C. W. W. Ng, Q. Mu, and C. Zhou, "Effects of soil structure on the shear behaviour of an unsaturated loess at different suctions and temperatures," Can. Geotech. J., vol. 53, pp. 589-601, 2016.

[9] J. T. Shahu, Yudhbir, and N. S. V. Kameswara Rao, "Effective stress behavior of quasi-saturated compacted cohesive soils," J. Geotech. Geoenviron. Eng., vol. 125, no. 9, pp. 772-781, 1999.

[10] D. G. Fredlund, H. Rahardjo, and M. D. Fredlund, Unsaturated Soil Mechanics in Engineering Practice. Hoboken, NJ, USA: John Wiley & Sons, Inc, 2012.

[11] R. Wu, G. Yang, S. Li, and Q. Xiang, "Experimental study on the effects of matric suction on shear properties of polypropylene fiber reinforced unsaturated clay," Materials, vol. 15, no. 24, p. 8223, 2022.

[12] H. Yokoi, "Relationship between soil cohesion and shear strength," Soil Sci. Plant Nutr., vol. 14, no. 3, pp. 89-93, 1968.

[13] S. K. Vanapalli, D. G. Fredlund, D. E. Pufahl, and A. W. Clifton, "Model for

the prediction of shear strength with respect to soil suction," Can. Geotech. J., vol. 33, no. 3, pp. 379-392, 1996.

[14] R. M. Imam, V. M. S. and M. J. S. "Shear strength of unsaturated sand at different relative densities," in Proc. 19th Int. Conf. Soil Mech. Geotech. Eng., Seoul, Korea, 2018, pp. 1-6.

[15] A. W. Bishop, "The principle of effective stress," Teknisk Ukeblad, vol. 106, pp. 859-863, 1959.

[16] M. N. & L. Laloui, "A unique relationship for shear strength determination of unsaturated soils," Geotechnique, vol. 48, no. 5, pp. 681-687, 1998.

[17] M. Nuth and L. Laloui, "Effective stress concept in unsaturated soils: Clarification and validation of a unified framework," Numer. Anal. Methods Geomech., vol. 32, no. 7, pp. 771-801, 2008.

[18] A. Öberg and G. Sällfors, "Determination of shear strength parameters of unsaturated silts and sands based on the water retention curve," Geotech. Test. J., vol. 20, no. 1, pp. 40-48, 1997.

[19] S. K. Vanapalli and D. G. Fredlund, "Shear strength of unsaturated soils and its applications in geotechnical engineering practice," Unsaturated Soils, vol. 1, pp. 3-50, 1997.

[20] J. W. Godt and N. Lu, "A closed-form equation for effective stress in unsaturated soil," Water Resour. Res., vol. 46, no. 5, p. W05515, 2010.

[21] A. Bouazza, J. M. Zornberg, and N. H. McCartney, "Significance of unsaturated behaviour of geotextiles in earthen structures," Aust. Geomech., vol. 41, no. 3, pp. 133-142, 2006.

[22] Y. S. J. M. Kim, H. I. K. Kim, and B. W. Oh, "Chemical extraction of arsenic from contaminated soil under subcritical conditions," Sci. Total Environ., vol. 409, no. 16, pp. 3076-3083, 2011.

[23] S. R. Pride, "Relationships between seismic and hydrological properties," in Hydrogeophysics. Berlin, Germany: Springer, 2005, pp. 253-290.

[24] G. Mavko, T. Mukerji, and J. Dvorkin, The Rock Physics Handbook. Cambridge, UK: Cambridge Univ. Press, 2020.

[25] D. J. Hornbaker, R. Albert, I. Albert, A. L. Barabási, and P. Schiffer, "What keeps sandcastles standing?," Nature, vol. 387, no. 6635, pp. 765-766, 1997.

[26] Z. Lu and J. M. Sabatier, "Effects of soil water potential and moisture content on sound speed," Soil Sci. Soc. Am. J., vol. 73, no. 5, pp. 1614-1625, 2009.

[27] G. Blight and A. W. Bishop, "Some aspects of effective stress in saturated and partly saturated soils," Geotechnique, vol. 13, no. 3, pp. 177-197, 1963.

[28] N. Lu, J. W. Godt, and D. T. Wu, "A closed-form equation for effective stress in unsaturated soil," Water Resour. Res., vol. 46, no. 4, p. W05515, 2010.

[29] A. Romero-Ruiz, N. Linde, L. Baron, S. G. Solazzi, T. Keller, and D. Or, "Seismic signatures reveal persistence of soil compaction," Vadose Zone J.,

vol. 20, no. 3, p. e204, 2021.

[30] J. Shen, J. M. Lorenzo, C. D. White, and F. Tsai, "Soil density, elasticity, and the soil-water characteristic curve inverted from field-based seismic P-and S-wave velocity in shallow nearly saturated layered soils," Geophysics, vol. 80, no. 3, pp. D183-D190, 2015.

[31] M. T. Van Genuchten, "A closed-form equation for predicting the hydraulic conductivity of unsaturated soils," Soil Sci. Soc. Am. J., vol. 44, no. 5, pp. 892-898, 1980.

[32] N. Lu and W. J. Likos, "Suction stress characteristic curve for unsaturated soil," Journal of Geotechnical and Geoenvironmental Engineering, vol. 132, no. 2, pp. 131-142, 2006.

[33] M. Nuth and L. Laloui, "Effective stress concept in unsaturated soils: Clarification and validation of a unified framework," International Journal for Numerical and Analytical Methods in Geomechanics, vol. 32, no. 7, pp. 771-801, 2008.

[34] J. Shen, J. M. Crane, J. M. Lorenzo, and C. D. White, "Seismic velocity prediction in shallow (<30 m) partially saturated, unconsolidated sediments using effective medium theory," Journal of Environmental & Engineering Geophysics, vol. 21, no. 1, pp. 67-78, 2016.

[35] R. Bachrach and P. Avseth, "Rock physics modeling of unconsolidated sands: Accounting for nonuniform contacts and heterogeneous stress fields in the effective media approximation with applications to hydrocarbon exploration," Geophysics, vol. 73, no. 6, pp. E197-E209, 2008.

[36] K. Š. L. a. P. P. Bláhová, "Influence of water content on the shear strength parameters of clayey soil in relation to stability analysis of a hillside in Brno region," Acta Universitatis Agriculturae et Silviculturae Mendelianae Brunensis, vol. 61, no. 5, pp. 1585-1594, 2013.

[37] ASTM, Standard Test Method for Consolidated Undrained Direct Simple Shear Testing of Cohesive Soils (ASTM D6528-07), West Conshohocken, Pennsylvania, United States: ASTM International, 2007.

[38] A. Zeybek, "Shaking table tests on seismic performance of shallow foundations resting on partially saturated sands," Arabian Journal of Geosciences, vol. 15, no. 1, pp. 12-20, 2022.

[39] J. K. Mitchell and K. Soga, Fundamentals of Soil Behavior, 3rd ed., Hoboken, New Jersey, United States: John Wiley & Sons, 2005.

[40] R. D. Holtz, W. D. Kovacs, and T. C. Sheahan, An Introduction to Geotechnical Engineering, 2nd ed., Upper Saddle River, New Jersey, United States: Pearson Prentice Hall, 2011.

[41] Z. Wang, J. Jia, L. Zhang, and Z. Li, "ViT-Based Image Regression Model for Shear-Strength Prediction of Transparent Soil," Buildings, vol. 14, no. 1, p. 9591, 2024.

[42] A. Arı, "Kum/Geotekstil Arayüzeyi Kayma Dayanımının Kesme Kutusu Deneyleriyle Belirlenmesi," Journal of the Faculty of Engineering and Architecture of Selcuk University, vol. 23, no. 2, pp. 123-136, 2008.

[43] ASTM, "The Place of the Direct Shear Test in Soil Mechanics," [Online]. Available: https://www.astm.org/PLACEHOLDER

[44] M. D. Bolton, "The Strength and Dilatancy of Sands," Geotechnique, vol. 36, no. 1, pp. 65-78, 1986.

[45] R. Khan and G. M. Latha, "Integrated Digital Image Analyses for Understanding the Particle Shape Effects on Sand–Geomembrane Interface Shear," International Journal of Geosynthetics and Ground Engineering, vol. 9, no. 3, pp. 1-11, 2023.

[46] P. Vangla and G. M. Latha, "Influence of Particle Size on the Friction and Interfacial Shear Strength of Sands of Similar Morphology," International Journal of Geosynthetics and Ground Engineering, vol. 1, no. 8, pp. 1-8, 2015.

[47] F. Daghistani and H. Abuel-Naga, "Evaluating the Influence of Sand Particle Morphology on Shear Strength: A Comparison of Experimental and Machine Learning Approaches," Applied Sciences, vol. 13, no. 6, p. 3591, 2023.

PUBLICATIONS FROM THE THESIS

Conference Papers

1. S. N. ALjalil & M. E. SELÇUK, “The Mechanical Behavior of Sand at a High Degree of Saturation”, International Congress of Engineering and Natural Sciences, 2023